

AD-A215 988

The Pennsylvania State University

The Graduate School

Carbon Black - Polyethylene Composites  
for PTC Thermistor Applications

A Thesis in  
Solid State Science

by

Lori Louise Rohlfing

Submitted in Partial Fulfillment  
of the Requirements  
for the Degree of

Master of Science

December 1987

DTIC  
ELECTE  
JAN 4 1990  
S B D

I grant The Pennsylvania State University the non-exclusive right to use this work for the University's own purposes and to make single copies of the work available to the public on a not-for-profit basis if copies are not otherwise available.

*Lori Louise Rohlfing*  
Lori Louise Rohlfing

DISTRIBUTION STATEMENT A

Approved for public release;  
Distribution Unlimited

20 01 04 111

We approve the thesis of Lori Louise Rohlfing.

Date of Signature:

July 24, 1987

Robert E. Newnham  
Robert E. Newnham, Alcoa  
Professor of Solid State  
Science, Chairman of Solid  
State Science, Thesis Advisor

July 24, 1987

A. S. Bhalla  
Amar S. Bhalla, -Professor of  
Solid State Science

July 28, 1987

James P. Runt  
James P. Runt, Associate  
Professor of Polymer Science

July 30, 1987

Wayne Huebner  
~~Wayne Huebner~~ Assistant  
Professor of Ceramic Science  
and Engineering

## ABSTRACT

Until recently, most PTC thermistors were composed of a rare-earth doped  $BaTiO_3$  composition. Now a new class of composite PTC thermistors are also commercially available. These composite thermistors exhibit a PTC measuring 6-8 orders of magnitude and have several advantages over conventional  $BaTiO_3$  thermistors, including lower room temperature resistivity, better thermal shock resistance, and high temperature stability.

In this study, composite PTC thermistors are produced from a carbon black/ polyethylene composition that exhibited a PTC of resistance measuring 6-8 orders of magnitude at  $125^\circ C$ . The composites are irradiated (gamma source) to induce polymer crosslinking. Crosslinking imparts mechanical integrity and prevents the onset of an NTC effect above the transition temperature. Crosslinking stabilizes the high temperature resistivity to  $200^\circ C$ . The electrical properties of these crosslinked composites are examined as functions of temperature, frequency, and thermal cycling.

To eliminate the crosslinking procedure, an insulating mullite phase was incorporated into the diphasic mixture to form a triphasic composite. Addition of the third filler yielded two effects. First, the filler provided sufficient mechanical stabilization of the composite structure to maintain high post-PTC resistance without an NTC effect. This mechanical stabilization

<input checked="" type="checkbox"/>	
<input type="checkbox"/>	
<input type="checkbox"/>	
<i>per form</i>	
Codes	
Dist	and/or
Special	
A-1	

persists to 200°C. The stabilization was accomplished without diminishing the magnitude of the PTC effect. The triphasic composites also displayed equivalent or better thermal cycling behavior than the diphasic composites.

Second, the addition of an insulating filler resulted in a shift of the room temperature resistivity caused by a shift in the percolation curve. The direction of shift of the percolation curve is dependent on the size difference between the conductor particles and the insulator particles. For insulating mullite particles approximately two orders of magnitude larger than the conducting carbon black particles, the curve shifted towards lower room temperature resistivities. When insulator particles are approximately the same size as the conductor particles, as illustrated in the  $V_2O_5$ - $Al_2O_3$ -polyethylene system, the percolation curve shifts towards higher room temperature resistivities.

This size dependence seems to indicate the presence of different connectivities. Equivalent sized particles form a 0-0-3 connectivity. Large differences in conductor and insulator particle size lead to the formation of quasi-composites, resulting in a 3(0-3)-0 connectivity.

Triphasic composites based on a carbon black-insulator-polyethylene system have proven to be a viable alternative to the crosslinked diphasic composites for use as a PTC thermistor.

TABLE OF CONTENTS

	Page
ABSTRACT.....	iii
LIST OF TABLES.....	vi
LIST OF FIGURES.....	vii
ACKNOWLEDGEMENTS.....	ix
 Chapter	
1 LITERATURE REVIEW.....	1
1.0 Introduction.....	1
1.1 Carbon Black.....	3
1.2 Composite Connectivity.....	4
1.3 Percolation and Conduction Mechanisms.....	7
1.4 PTC Effect in Conductor-Loaded Composites...	12
1.5 Crosslinking.....	17
1.6 Thermistor Properties.....	22
1.7 Goals of Research.....	24
2 EXPERIMENTAL PROCEDURE.....	26
2.1 Characterization of Starting Materials.....	26
2.2 Sample Preparation.....	30
2.3 Composite Characterization.....	35
2.4 Electrical Resistance Measurements.....	40
2.5 High Power Testing.....	45
3 RESISTIVITY MEASUREMENTS - PERCOLATION.....	47
3.1 Percolation in Diphasic Composites.....	48
3.2 Percolation in Triphasic Composites.....	51
4 RESISTIVITY MEASUREMENTS - PTC EFFECT.....	68
4.1 PTC Effect in Diphasic Composites.....	68
4.2 PTC Effect in Triphasic Composites.....	72
4.3 Thermal Cycling.....	77
4.4 High Power Testing.....	89
4.5 High Frequency Measurements.....	90
5 SUMMARY.....	94
5.1 Conclusions.....	94
5.2 Future Work.....	97
REFERENCES.....	98

## LIST OF TABLES

Table		Page
2.1.1	Particle Characteristics of Starting Powders.....	29
2.3.1	Comparison of Geometric and Theoretical Densities of Diphasic Composites.....	37
2.3.2	Comparison of Geometric and Re-calculated Theoretical Densities of Diphasic Composites....	38
2.3.3	Comparison of Geometric and Theoretical Densities of Triphasic Composites.....	39
2.3.4	Comparison of Geometric and Re-calculated Theoretical Densities of Triphasic Composites....	41
4.3.1	Typical Recovery Properties.....	8.

## LIST OF FIGURES

Figure	Page
1.2.1 Connectivity Models for Diphasic Composites.....	5
1.3.1 Illustration of Percolation.....	8
1.4.1 Connectivity Transition During PTC Effect.....	14
1.4.2 Major Types of Resistivity-Temperature Curves....	15
1.5.1 Resistivity-Temperature Curve for Various Degrees of Crosslinking.....	19
1.5.2 Resistivity-Temperature Curves for Crosslinked and Not Crosslinked Composites on Heating and Cooling.....	20
1.5.3 Reproducibility of Resistivity-Temperature Curve for Crosslinked and Not Crosslinked Composites...	21
2.1.1 Outline of Sample Preparation.....	27
2.1.2 Scanning Electron Micrographs of Carbon Black....	28
2.1.3 Scanning Electron Micrographs of Mullite Zeospheres.....	31
2.1.4 Scanning Electron Micrographs of A-14 Alumina and AKP-30 Alumina Powders.....	32
2.3.1 Scanning Electron Micrographs of a Diphasic Composite.....	42
2.3.2 Scanning Electron Micrographs of a Triphasic Composite.....	43
3.1.1 Percolation Curve for Uncrosslinked Composites...	49
3.1.2 Comparison of Crosslinked and Uncrosslinked Percolation Curves.....	50
3.2.1 Percolation Curve for Triphasic Carbon Black Composites.....	52
3.2.2 Percolation Curve for Triphasic $V_2O_3$ Composites.....	53
3.2.3 Schematics of 0-0-3 and 3(0-3)-0 Composite Connectivities.....	55

3.2.4	Effect of Carbon Black/Polyethylene Ratio on the Resistivity of Carbon Black Composites.....	58
3.2.5	Model for Theoretical Calculation of Triphasic 3(0-3)-0 Composite Resistivity.....	60
3.2.6	Theoretical Predictions of Percolation Curves for a 3(0-3)-0 Composite.....	62
3.2.7	Comparison of Theoretical and Experimental Percolation Curves for a 3(0-3)-0 Composite.....	63
3.2.8	Effect of Insulator Particle Size on Resistivity of Carbon Black Composites.....	66
4.1.1	Resistivity-Temperature Curves for Uncrosslinked Composites.....	70
4.1.2	Resistivity-Temperature Curves for Crosslinked Composites.....	71
4.2.1	Resistivity-Temperature Curves for Triphasic Composites.....	74
4.2.2	Resistivity-Temperature Curves for Triphasic Composites with Different Size Fillers.....	76
4.3.1	Heating-Cooling Curve for Uncrosslinked Sample...	79
4.3.2	Heating-Cooling Curve for Crosslinked Sample.....	80
4.3.3	Heating-Cooling Curve for Triphasic Sample.....	82
4.3.4	Multiple Heating Curves for a Crosslinked Composite.....	83
4.3.5	Multiple Heating Curves for a Triphasic Composite	84
4.3.6	Multiple Heating Curves for a Triphasic Composite	86
4.5.1	Resistivity-Temperature Curve for a Crosslinked Diphasic Composite at Various Frequencies.....	92
4.5.2	Resistivity-Temperature Curve for a Triphasic Composite at Various Frequencies.....	93

## ACKNOWLEDGEMENTS

I would like to express my deep appreciation and thanks to R.E. Newnham for his insight, guidance, and support throughout this thesis investigation. I would also like to thank Dr. J.P. Runt and Arvind Halliyal for their advice and guidance during the course of my thesis research. Sincere gratitude is also extended to Steven M. Pilgrim whose vast experience with composites and polymers was invaluable to this investigation. Also, thanks go to all my office mates, Craig Nies, Ruyan Guo, Joe Kearns, and Umesh Kumar for their constant encouragement and for making time at in the office more enjoyable. Special thanks goes to my husband Rick for his support, encouragement, and understanding throughout this project.

Funding for this study was provided by the National Science Foundation and the Office of Naval Research.

## CHAPTER 1

### LITERATURE REVIEW

#### 1.0 INTRODUCTION

Following a trend that started in the aerospace and semiconductor industries, material scientists are no longer as much concerned with the properties of the best single phase materials, but instead are trying to enhance or improve properties using composites. Composites are a combination of phases, selected for their best individual properties, which are put together in such a way as to optimize overall behavior. This means that it is not only important to study the properties of the phases individually, but also to study the ways in which the phases are combined.

A great deal of work is presently being done to optimize the electrical properties of composite materials and explore new applications. One such interesting composite is composed of a highly conducting carbon black phase dispersed in an insulating polymer matrix phase. This type of composite has applications as conductive coatings, temperature sensors, electromagnetic induction shielding, force sensing resistors, and, as in the case of this study, Positive Temperature Coefficient (PTC) thermistors.

PTC thermistors are used as temperature sensors, flow meters, and to provide protection to circuitry from voltage

surges and current overloads. When heated to a certain critical temperature, a PTC material will rapidly "switch" from a conducting state to a non-conducting state. PTC devices function similar to a fuse, except that a fuse must be replaced after each use whereas a thermistor can be switched numerous times.

Currently, most PTC thermistors produced are a rare earth doped BaTiO<sub>3</sub> composition. BaTiO<sub>3</sub> thermistors consist of semiconducting grains surrounded by insulating grain boundaries. The PTC effect occurs when the BaTiO<sub>3</sub> reaches its Curie temperature, where a ferroelectric to paraelectric phase transition occurs that results in changes in the potential barrier at the grain boundary. Commercially produced BaTiO<sub>3</sub> thermistors exhibit PTC's of 3-5 orders of magnitude, but have high room temperature resistivities, approximately 100  $\Omega$ -cm. The fabrication of these ceramic thermistors is costly and requires complex processing.

Recently, Raychem Corporation has begun production of a carbon black-polyethylene composite PTC thermistor which exhibits several advantages over conventional BaTiO<sub>3</sub> devices. The advantages of the composite thermistor include a PTC effects measuring 6-8 orders of magnitude, better thermal shock resistance, lower room temperature resistivity, and voltage independent PTC behavior.<sup>(1)</sup> Also, these composite thermistors are able to maintain high resistivities at temperatures well above the PTC transition

temperature, whereas  $BaTiO_3$  thermistors display NTC behavior at temperatures above the transition.

### 1.1 CARBON BLACK

Carbon blacks are typically composed of nearly pure carbon in colloidal entities of aciniform morphology. Aciniform means "clustered-like grapes" and refers to the characteristic appearance of the spherical particles fused together in clusters of branched, irregular shapes, generally called aggregates. The carbon atoms are arranged in imperfect graphite layers within each aggregate.<sup>(2)</sup>

The aciniform morphology makes accurate measurement of particle diameter very difficult, if not impossible. Also, the substantial loss of surface area resulting from the fusion of particles makes particle size and surface area determination difficult.<sup>(3)</sup>

Carbon blacks contain small amounts of hydrogen and oxygen on the surface of the particles. The hydrogen and oxygen attach as functional groups to the edge of defect carbon atoms in the graphitic layers of the aggregate. The oxygen groups have a pronounced effect on the electrical conductivity, the adsorption of moisture, and on interactions with other materials. These groups act as electron traps and thus decrease the conductivity.

Different grades of carbon black are distinguished

mainly by their surface area, structure, and surface chemistry. High surface area, high porosity, highly structured carbon blacks with few or no adsorbed oxygen or hydrogen groups are the best conductors. Highly structured refers to the highly extended, bulky nature of the aggregates. This, coupled with a high degree of porosity, contributes strongly to network formation and thus to high conductivity.

## 1.2 COMPOSITE CONNECTIVITY

Composites, simply restated, are a combination of phases selected for their best individual properties, which are put together in such a way as to optimize the desired properties. For this reason, it is important to examine the ways in which the phases are connected, or in other words, the connectivity of the phases. The connectivity a composite exhibits is crucial in determining the behavior of that composite.

Connectivity may be defined as the number of dimensions in which a phase is self-connected.<sup>(4)</sup> Within a composite, each phase may be connected to itself in zero, one, two, or three dimensions, corresponding to three perpendicular axes. Rules of precedence determine the order in which the constituent phases are written.<sup>(5)</sup>

In diphasic composites, sixteen possible connectivity patterns exist. Ten of these are shown in figure 1.2.1. The

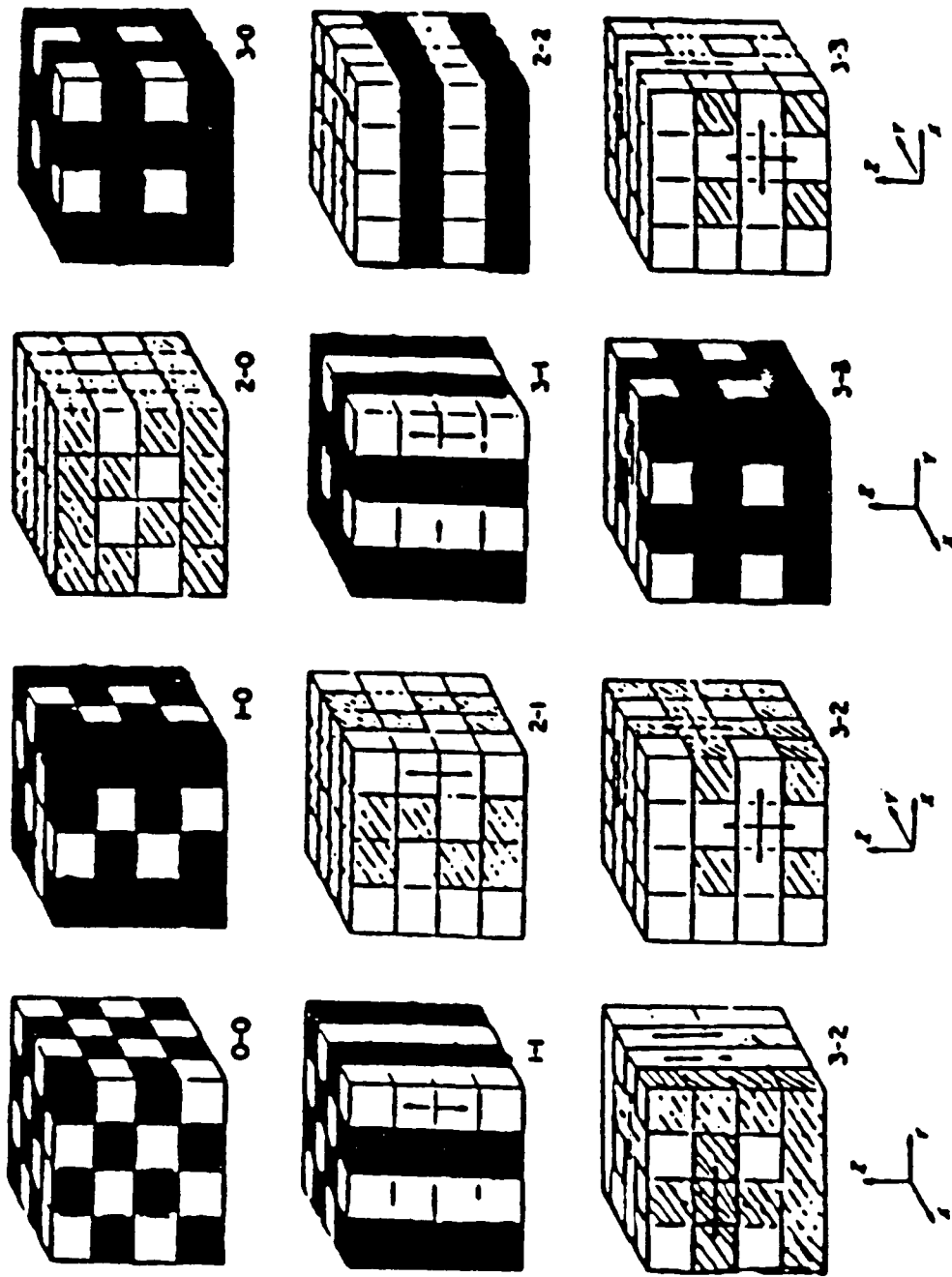


Figure 1.2.1 Connectivity Models for Diphasic Composites.

ten differ in complexity from the simple 0-3, which corresponds to particles completely surrounded by a matrix, to the complex 3-3, where both phases are self-connected in all three dimensions.

In the case of a three component composite, 64 different connectivity patterns are possible. For example, a 0-0-3 composite would consist of two different particulate phases of approximately the same size dispersed throughout a third, continuous matrix phase. In addition to the 64 triphasic connectivity patterns, three or more component composites may form quasi-composites.<sup>(6)</sup>

Quasi-composites may be described as a composite within a composite. A quasi-composite is formed when one phase is entirely within another phase, or when the composite constituents are very different in size. An example of quasi-composite formation would be PZT rods (A), embedded in a polymer matrix (B), with a particulate conductor (C) dispersed throughout the matrix. Since the particulate conductor is much smaller than the PZT rods, a quasi-composite (B-C) is formed between the conductor and the matrix with 0-3 connectivity. The quasi-composite (B-C) is three dimensionally connected and the PZT rods one-dimensionally connected in the total composite. Following the rules of precedence for composite nomenclature, the active phase listed first, the total composite connectivity is written 1-3(0-3). The total composite connectivity is pseudo-diphasic, comprised of a

one-dimensionally connected PZT rods phase, the active phase, and the three dimensionally connected polymer/conductor quasi-composite.

The connectivity pattern present is particularly important to the electrical properties of a composite. When a particulate conducting filler is dispersed in an insulating matrix, the type of connectivity present determines the conduction behavior of the composite. In turn, the percolation behavior of the composite determines the type of connectivity that will exist.

### 1.3 PERCOLATION and CONDUCTION MECHANISMS

It has been well documented (1-3,7-11) that the electrical resistivity of an insulating polymer filled with conducting particles, such as metal or carbon black, experiences a sharp decrease in resistivity at a critical filler concentration or percolation threshold concentration. It has become a common proposition that this sharp transition is the result of the filler particles coming into contact with each other and forming a chain-like structure which provides a continuous conduction path. This transition is illustrated in figure 1.3.1 for a conducting filler ( $\rho_{\text{filler}} = 10^{-6} \Omega\text{-cm}$ ) in an insulating polymer matrix ( $\rho_{\text{matrix}} = 10^{16} \Omega\text{-cm}$ ). (11)

Below the percolation limit, the conducting particles are isolated by the insulating polymer matrix phase (0-3

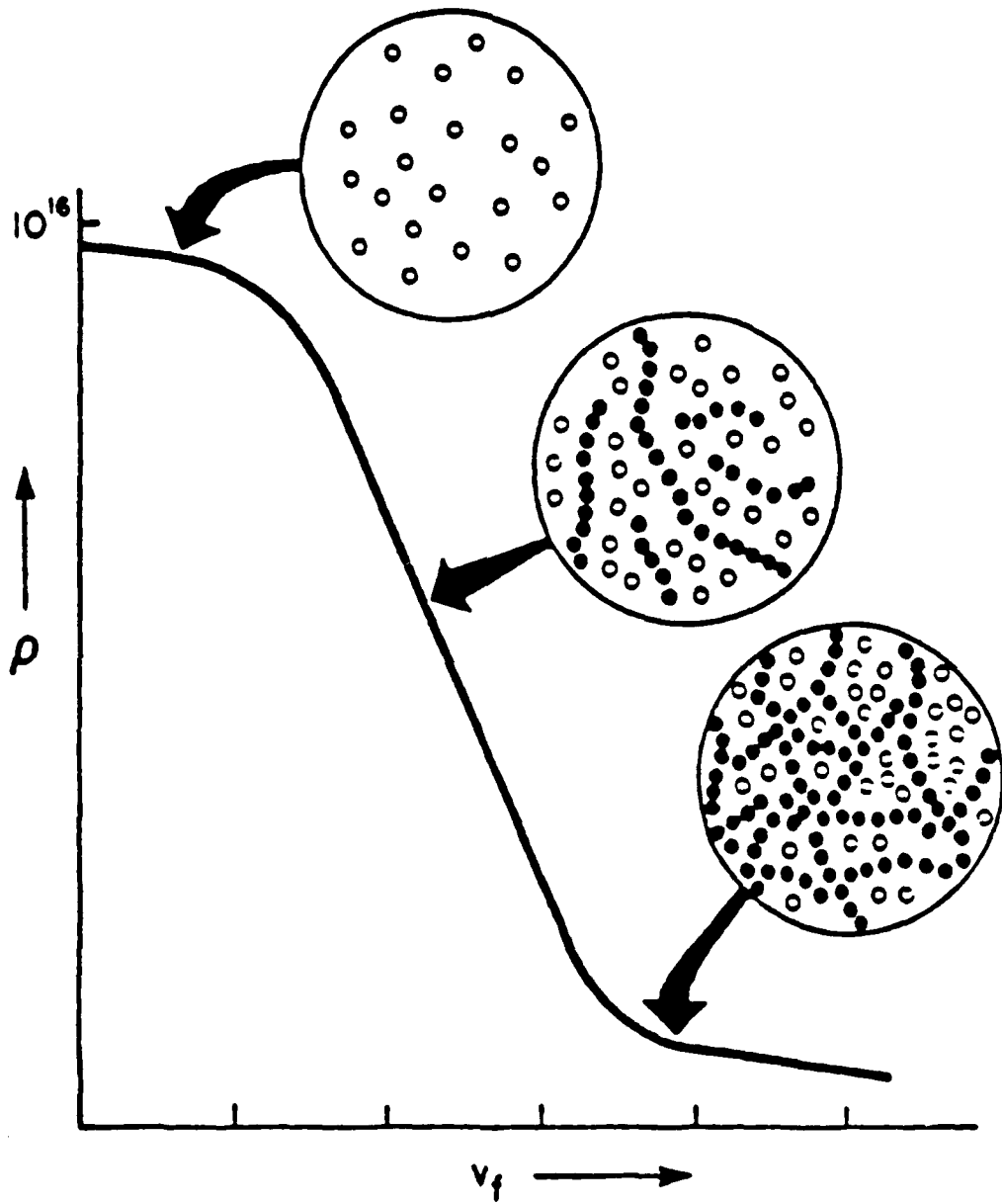


Figure 1.3.1 Illustration of Percolation.

connectivity) so that the composite exhibits a high resistivity. By increasing the concentration of conducting particles, the particles become closer to each other, resulting in a slight decrease in the resistivity of the material due to electron tunneling.

As the concentration of the conductive filler is further increased, a critical concentration or threshold concentration is reached. At the threshold concentration, the conducting particles form an uninterrupted conduction path and behave similarly to filaments of the conducting material (3-3 connectivity).

The average chain length of contacting filler elements continues to increase as the concentration of conducting filler increases up to the saturation concentration. At the saturation concentration extensive chain branching results in network formation of conduction paths. Once this continuous conduction network forms, the behavior of the composite is controlled by the highly conducting filler material and the composite exhibits a very low resistivity. Increasing the filler concentration beyond the saturation concentration only leads to a slight decrease in resistivity since additional particles merely fill in the interstices of the network.

Many factors are known to influence the percolation curve, such as the choice of filler material, the particle size, shape, size distribution, aggregation level of the filler, uniformity of dispersion, and the nature of the host

polymer matrix. For instance, conductive carbon blacks exhibit percolation thresholds far below theoretical predictions for spherical metal powders dispersed in polymers. This can be attributed to the unique aggregate structure of carbon black that promotes the formation of conducting networks.<sup>(12)</sup>

The nature of the host polymer matrix is also very important in determining the percolation threshold. Semi-crystalline polymers tend to concentrate the very small carbon black aggregates in the amorphous regions. During polymer crystallization, a major portion of the carbon black aggregates are preferentially excluded from crystalline regions and are forced into inter-spherulitic boundaries or into amorphous regions within the spherulites. Consequently, semi-crystalline polymers exhibit a lower threshold percolation concentration than amorphous polymer.<sup>(12)</sup>

The critical threshold concentration of carbon black is not only dependent on the degree of crystallinity of the polymer, but also on the surface tension of the polymer. This dependence was explained by a simple model.<sup>(13)</sup> The model predicts that when the interfacial excess energy introduced by carbon particles in the polymer matrix reaches a "universal value",  $\Delta g^*$ , the carbon particles begin to flocculate in order to avoid any further increase in energy and to form networks which facilitate electrical conduction.

Many mathematical models for percolation have been proposed<sup>(7-14)</sup>, the majority of which are derived for

specific systems. The difficulty in deriving a general model lies in incorporating the many varied qualitative composite parameters, such as degree of agglomeration of filler, particle geometry, and polymer characteristics, into a quantitative expression.

The electrical conductivity of a composite is not controlled by percolation behavior only. Many other factors which affect conductivity have been proposed, the most common being electron tunneling and thermal expansion.<sup>(3, 14-18)</sup> Electron tunneling is important at filler concentrations below and slightly above the threshold concentration. It occurs when conductive particles are close to each other but are not contacting each other. When the distance separating the conducting particles ( $l_g$ ) is small (less than  $100 \text{ \AA}$ ), electrons may quantum-mechanically tunnel through the narrow insulating gaps to other conducting particles, resulting in a lower resistivity of the composite than normally would be expected.

The tunneling current that exists across the gap is exponentially dependent on the gap width. In addition to the contribution of the tunneling current to the voltage across the junction, there exists an induced voltage resulting from quantum thermal fluctuations. When the capacitance of the junction is small, which is generally the case in these composites, the induced voltage can be an appreciable portion of the total voltage on the junction.<sup>(3)</sup>

At high temperatures, the tunneling current can

increase because thermal fluctuations lower the potential barrier between carbon aggregates. But at high temperatures, a directly competing effect becomes important, that being the expansion of the polymer widening the gaps between carbon aggregates.

Thermal expansion coefficients of polymers are generally considerably larger than those for the metallic-like conducting fillers. Consequently, changes in temperature will result in changes in the distance between conductive particles ( $lg$ ) due to the expansion of the polymer. Increasing the interparticle distance will produce a decrease in the conductivity of the composite.

#### 1.4 PTC EFFECT IN CONDUCTOR-LOADED POLYMER COMPOSITES

When crystalline polymers are heated to near their melting temperature, they exhibit a small increase in volume and therefore a slight increase in resistivity due to their high coefficient of thermal expansion. When the melting temperature is reached, the polymer will undergo a large, discontinuous volume increase that results from the crystalline to amorphous phase transition. This large volume expansion of the polymer pulls the conducting filler particles apart thus destroying the continuous conduction pathways and causing the resistivity of the composite to dramatically increase by several orders of

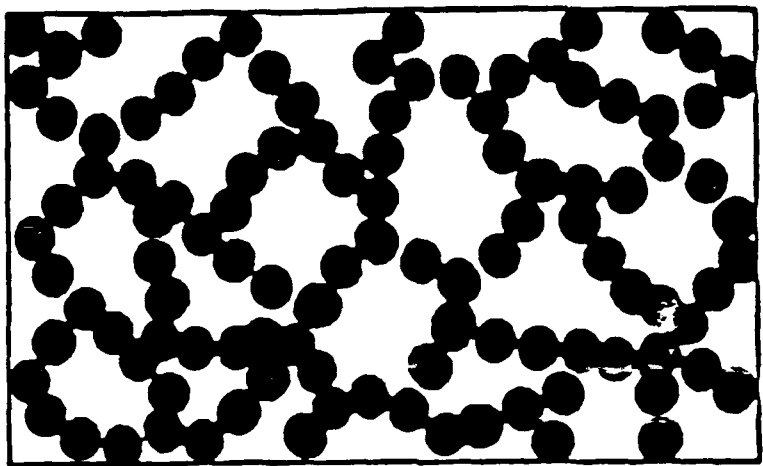
magnitude.<sup>(12, 14-17)</sup> This large increase in resistivity with temperature is known as the Positive Temperature Coefficient (PTC) of resistance effect. In terms of connectivity, the composite switches from a (3-3) type connectivity to a (0-3) type of connectivity [figure 1.4.1].

Many different conductor-loaded polymer systems exhibit a PTC effect. A variety of conductive fillers have been studied, including  $V_2O_5$ , TiO, Ni, Al and Ag.<sup>(12-15)</sup> At the present time, the most widely studied systems are the carbon black loaded polymer systems.

The electrical resistivity versus temperature relationship of carbon black dispersed in different polymeric materials can be represented by three major types of effects. These three types of effects are illustrated in figure 1.4.2, and include a Negative Temperature Coefficient (NTC), a Low Positive Temperature Coefficient (L-PTC), and a High Positive Temperature Coefficient (H-PTC) of resistance. The type of effect a given carbon black-polymer composite will display depends largely on the degree of crystallinity of the polymer. Highly crystalline polymers generally show a large PTC of resistance, unlike amorphous polymers that show little or no PTC of resistance when loaded with carbon black.<sup>(2, 26)</sup>

The concentration of conductive filler will also affect the magnitude of the PTC. Maximum changes in resistivity are obtained with conductor loadings near the percolation threshold concentration. It is here that the conducting

### 3-3 CONNECTIVITY



- CARBON BLACK
- POLYETHYLENE

### 0-3 CONNECTIVITY

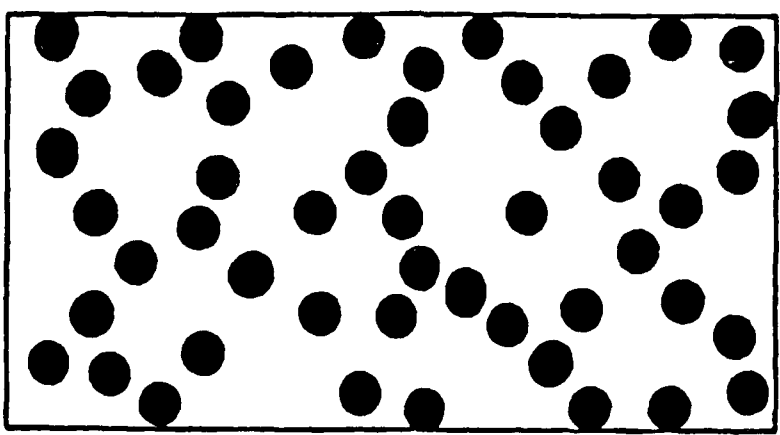


Figure 1.4.1 Connectivity Transition During PTC Effect.

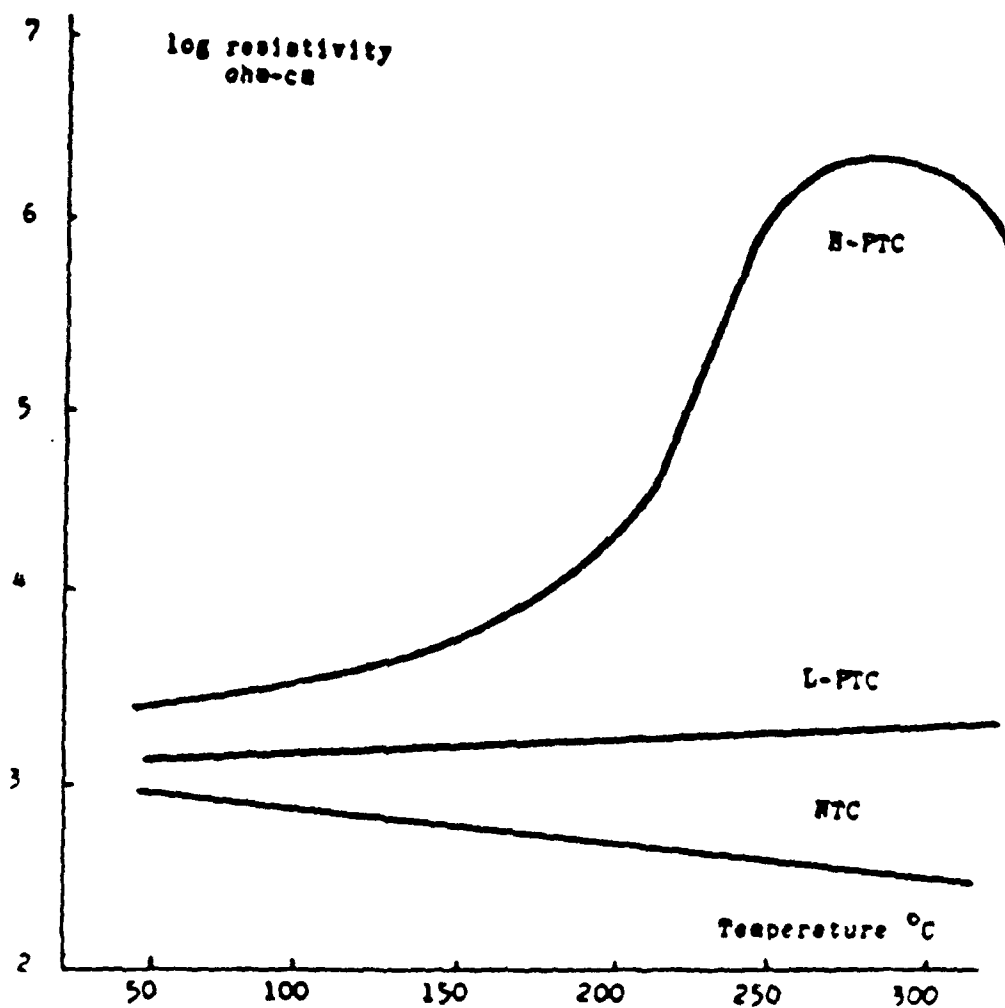


Figure 1.4.2 Major Types of Resistivity-Temperature Curves.

particles have just come into contact with each other to form the conducting pathways and so the expansion of the polymer will more completely dissociate the particles, giving the greatest possible change in resistivity.

Carbon black filled polymers behave in accordance with the conduction and percolation models for conductor-filled polymers, the only difference being that carbon black particles seldom exist separately. They are usually fused into aggregates, and these aggregates have a tendency to join and form loosely bound agglomerates due to Van der Waals forces. Shear, vibrational, or thermal disturbances will easily break up the agglomerates into the original aggregates. This process is known as deagglomeration.

Deagglomeration occurs as the temperature of the composite is increased due to an increase in Brownian particle motion, which in turn is a result of both the increase in temperature and the reduction in viscosity of the polymer.<sup>(26)</sup> This process leads to a slight increase in the distance between particles and thus a slight increase in resistivity. However, the most important changes in the composite with temperature occur at the melting temperature of the polymer.

Semi-crystalline polymers consist of a crystalline phase embedded in an amorphous phase. When carbon black is added to a semi-crystalline polymer, the particles are entirely restricted to the amorphous phase. When the temperature of the mixture enters the melting range, a major

rearrangement of the carbon black particles will occur as the crystalline phase disappears and the matrix becomes a homogeneous amorphous phase with a larger volume. [26, 27] The result is a large PTC in the resistivity of the composite at the melting temperature.

Non-crystalline polymers generally show a low, if any, PTC effect. The low PTC effect observed in amorphous polymers is due to the increase in interparticle distance as a result of deagglomeration. [26].

### 1.5 CROSSLINKING

Although carbon black loaded polymer composites exhibit a substantial PTC at the polymer melting temperature, their usefulness is limited by the onset of an NTC immediately following the PTC. [28] Since the PTC is a consequence of the polymer crystallites melting into an amorphous phase, the NTC phenomenon is caused by the movement of the conducting particles or aggregates in the less viscous, molten polymer to form a new distribution of better uniformity and conductivity. [29, 31, 32]

One method used to eliminate the deleterious NTC effect is to crosslink the polymer. Crosslinking refers to the "cross-bonding" or interlinking of the rows of polymer chains. By crosslinking the polymer, the structure of the polymer network is stabilized and the movement of the carbon

particles is greatly reduced without sacrificing the PTC effect. (20, 21, 27)

As seen in figure 1.5.1, composites consisting of a carbon black-polyethylene mixture that are not crosslinked exhibit a large NTC following the PTC. However, composites that have been crosslinked maintain their high resistivity at temperatures well above the melting temperature of the polymer. The one drawback to crosslinking is that a moderate increase in room temperature resistivity occurs. (27)

When a thermoplastic or uncrosslinked composite is repeatedly subjected to heating and cooling cycles, the accompanying expansion and contraction processes in the composite cause movement of the carbon particles and aggregates without returning them to their original position. As a result, the thermoplastic composite displays poor electrical reproducibility [figure 1.5.2b]. But when the composite structure is stabilized by crosslinking, the movement of the carbon particles is sufficiently reduced to enable the carbon particles to return to their original position. Figure 1.5.2a illustrates the good reproducibility of the resistivity versus temperature curve displayed by crosslinked composites. Only the first heating cycle differs from the subsequent cycles, and this is due to differences in thermal history.

Figure 1.5.3 shows a complete heating and cooling cycle. The cooling curve of a crosslinked composite is just an approximate shift of the heating curve along the

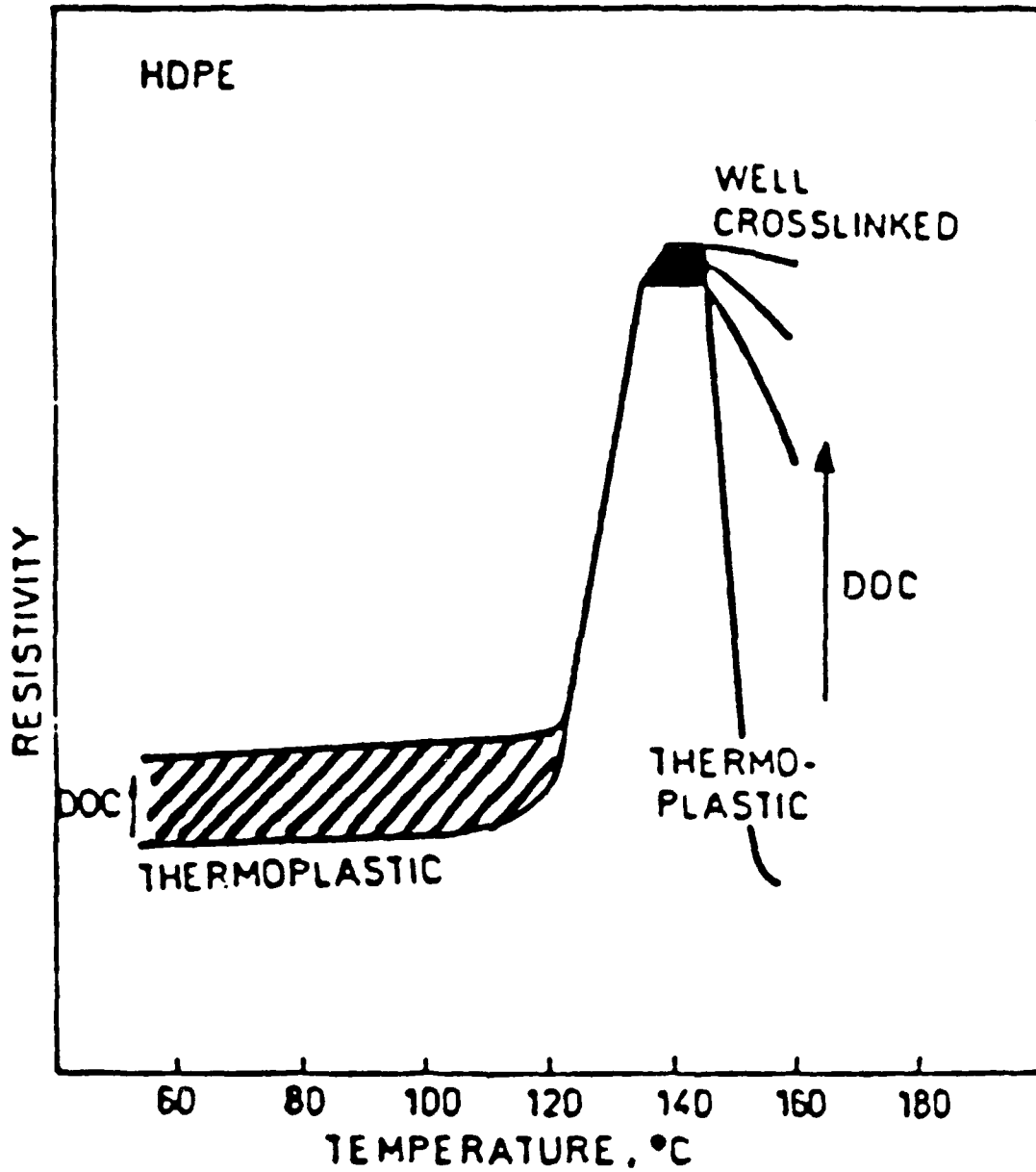


Figure 1.5.1 Resistivity-Temperature Curve for Various Degrees of Crosslinking.

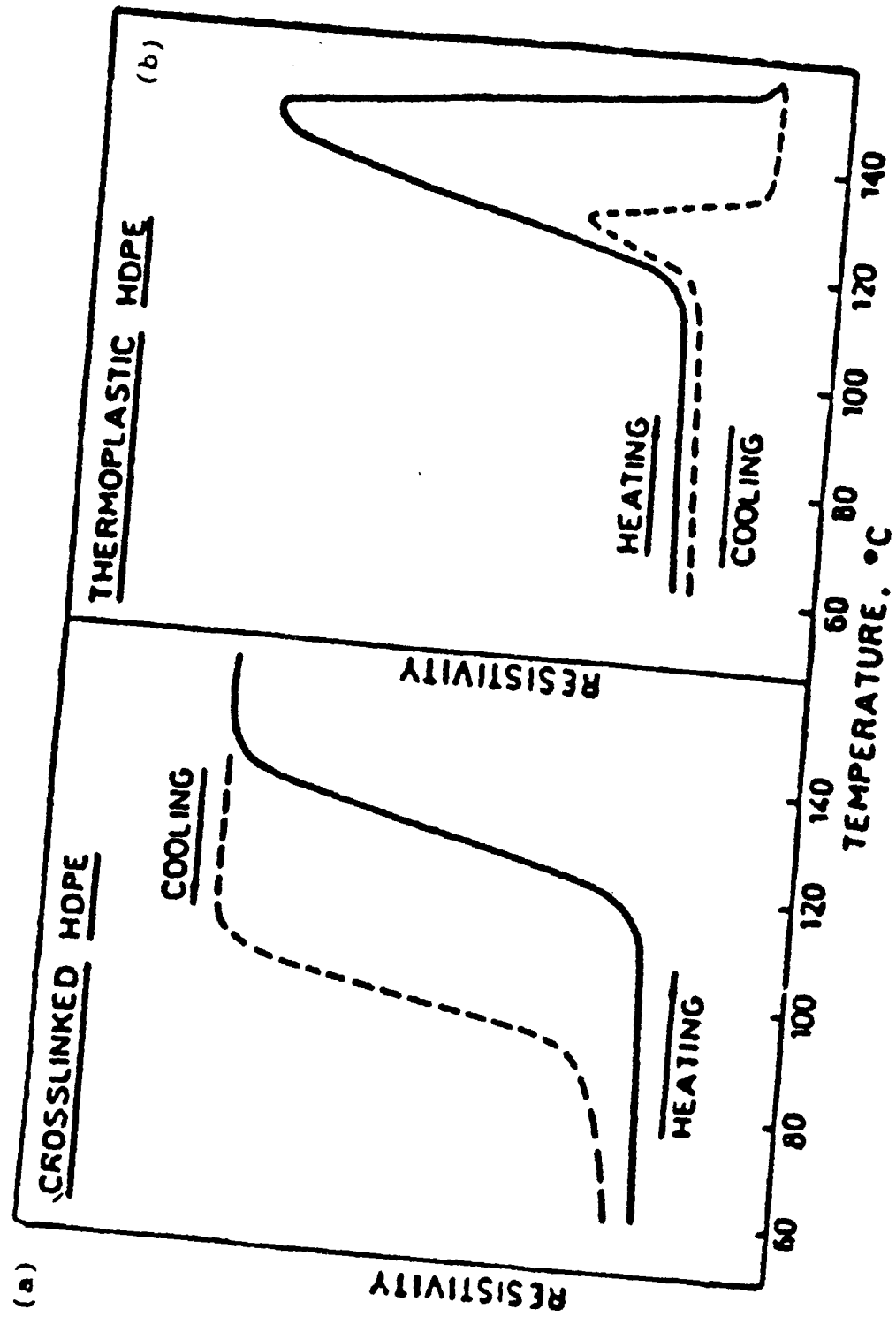


Figure 1.5.2 Resistivity-Temperature Curves for (a) Crosslinked and (b) Not Crosslinked Composites on Heating and Cooling.

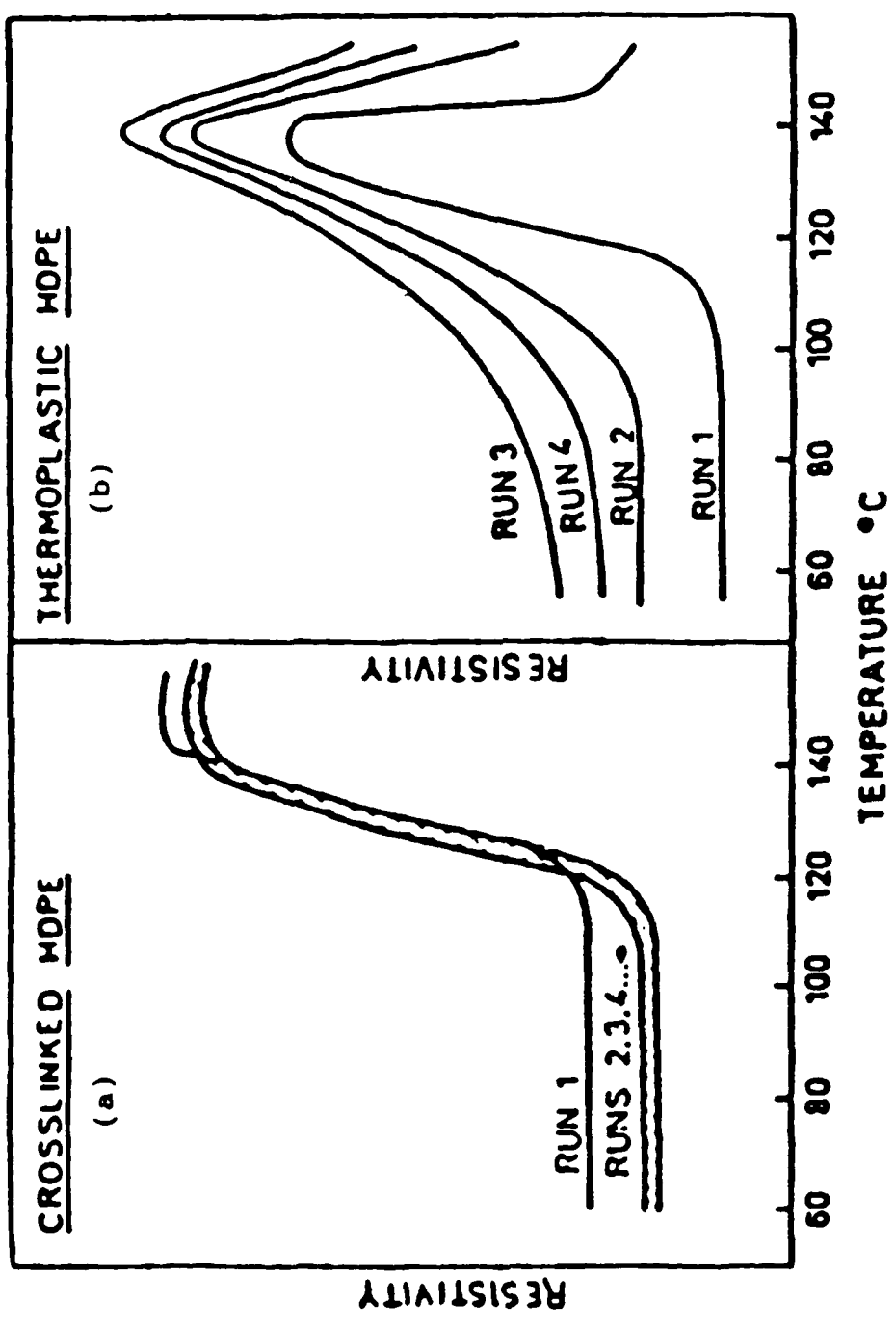


Figure 1.5.3 Reproducibility of Resistivity-Temperature Curve for (a) Crosslinked and (b) Not Crosslinked Composites.

temperature axis. This hysteresis on cooling is inherent to all polymers, for the crystallization temperature of a polymer is lower than the melting temperature and the kinetics of polymer crystallization are slow.

The stabilization of the polymer network structure at high temperatures is critical to the practical application of these PTC materials. Earlier attempts to overcome the NTC and reproducibility problems involved adding rubber as a mechanical stabilizer to carbon/wax mixtures<sup>(29)</sup>, or by using mixtures of two different carbon blacks in polyethylene.<sup>(30)</sup> Although some improvements in the reproducibility were achieved, they were insufficient for practical application. The best solution thus far has been crosslinking of the polymer.<sup>(27)</sup>

Crosslinking can be induced either chemically or by irradiation of the composite. The chemical process is complicated and involves a heat treatment, and the irradiation method is very costly. Better results seem to be obtained by radiation induced crosslinking.<sup>(20, 21)</sup>

## 1.6 THERMISTOR PROPERTIES

The final desired properties of a PTC thermistor must be considered when deciding on certain processing variables such as the amount of carbon black, the choice of polymer, and the degree of crosslinking. The choice of polymer will determine the temperature at which the PTC will occur and,

depending on the degree of crystallinity, the magnitude of the PTC effect. The amount of carbon will determine the room temperature resistivity and the magnitude of the PTC within a given polymer. The degree of crosslinking will also affect the room temperature resistivity, as well as the high temperature PTC behavior.

Several key features desired in a PTC thermistor include: [1, 2, 3]

- 1) lowest possible room temperature resistivity
- 2) largest PTC effect possible
- 3) ability to maintain high resistivity above  $T_m$  of polymer
- 4) good reproducibility on thermal cycling
- 5) rapid recovery time
- 6) good power handling capabilities

However, several of these desirable features are diametrically opposed to each other.

This is the case with the room temperature resistivity and the magnitude of the PTC effect. To decrease the room temperature resistance, more carbon is added. But by adding more carbon, the magnitude of the PTC is lowered. A similar situation exists when trying to maintain high resistivity at elevated temperatures and still preserve the lowest possible

room temperature resistance. Crosslinking imparts high temperature stability, but also increases the room temperature resistance.

One disadvantage of the Raychem Polyswitch and other composite thermistors is the slow recovery time.<sup>(1,28,31)</sup> The slow recovery of the base resistance is due to secondary recrystallization of the polymer and gradual reformation of the carbon black chains. The thermistor starts at some initial resistance termed the minimum base resistance. After the first cycle of heating to 130°C and cooling to room temperature, the new resistance  $R(1)$  is 20% higher than the initial resistance. This is called the maximum base resistance. Even after 24 hours, the resistance  $R(24)$  is still 15% above the initial resistance. Subsequent heating cycles return to a base resistance approximately equal to the maximum base resistance  $R(1)$ .<sup>(1,28)</sup>

When producing composite PTC thermistors, all of these factors must be taken into consideration. The final composition will depend on which parameters are most important for a specific application.

## 1.7 GOALS OF RESEARCH

Carbon black-loaded polymer composites show great potential for a variety of applications. As a PTC thermistor, they offer many advantages over conventional

BaTiO<sub>3</sub> thermistor materials for use as overcurrent protectors, temperature sensors, and flow meters.

The focus of this study will be carbon black-polyethylene composites for PTC thermistor applications. To begin, crosslinked carbon black-polyethylene composites will be produced in order to verify previous results by Raychem and others, as well as gain experience in the processing and property measurement techniques required to produce and characterize these materials.

Next, ways of improving both the processing and properties of these thermistors will be investigated. In particular, a way to produce a suitable thermistor material that eliminates the need to crosslink the polymer would be especially desirable.

Additionally, the effects that a third, non-conducting phase introduced into the diphasic carbon black-polyethylene composite would have on both the percolation and PTC behavior will be explored. The possibility of using this third component to stabilize the structure and thus eliminate the need to crosslink will be examined.

Lastly, the new types of connectivity patterns formed by the additions of a third phase will be determined, the possibility of quasi-composite formation explored, and a correlation among the percolation and PTC behavior and the new triphasic connectivity patterns will be discussed.

## CHAPTER 2

### EXPERIMENTAL PROCEDURE

To achieve the goals set forth in this study, two basic types of composite samples were needed: the diphasic carbon black and polyethylene, and the triphasic carbon black, polyethylene, and insulator  $Al_2O_3$  or mullite phase. The preparation sequence is virtually the same for both types of composites, and is outlined in Figure 2.1.1.

#### 2.1 CHARACTERIZATION OF STARTING MATERIALS

The carbon black utilized throughout this study was a Sterlings N.S. (Cabot Corporation) with an average particle size of 0.075  $\mu m$  estimated from BET surface area. Scanning electron micrographs of the carbon black in Figure 2.1.2 illustrate the minute size and spherical shape, as well as the high degree of agglomeration present.

Marlex 6001 high density polyethylene (Phillips Chemical Company) was designated as the matrix material for these composites. This polyethylene, manufactured in bead form, has a melting temperature of 130°C and a density of 0.965  $g/cm^3$ .<sup>(33)</sup>

When preparing the triphasic samples, three different insulating powders of different sizes and shapes were used (Table 2.1.1). A major portion of the triphasic samples

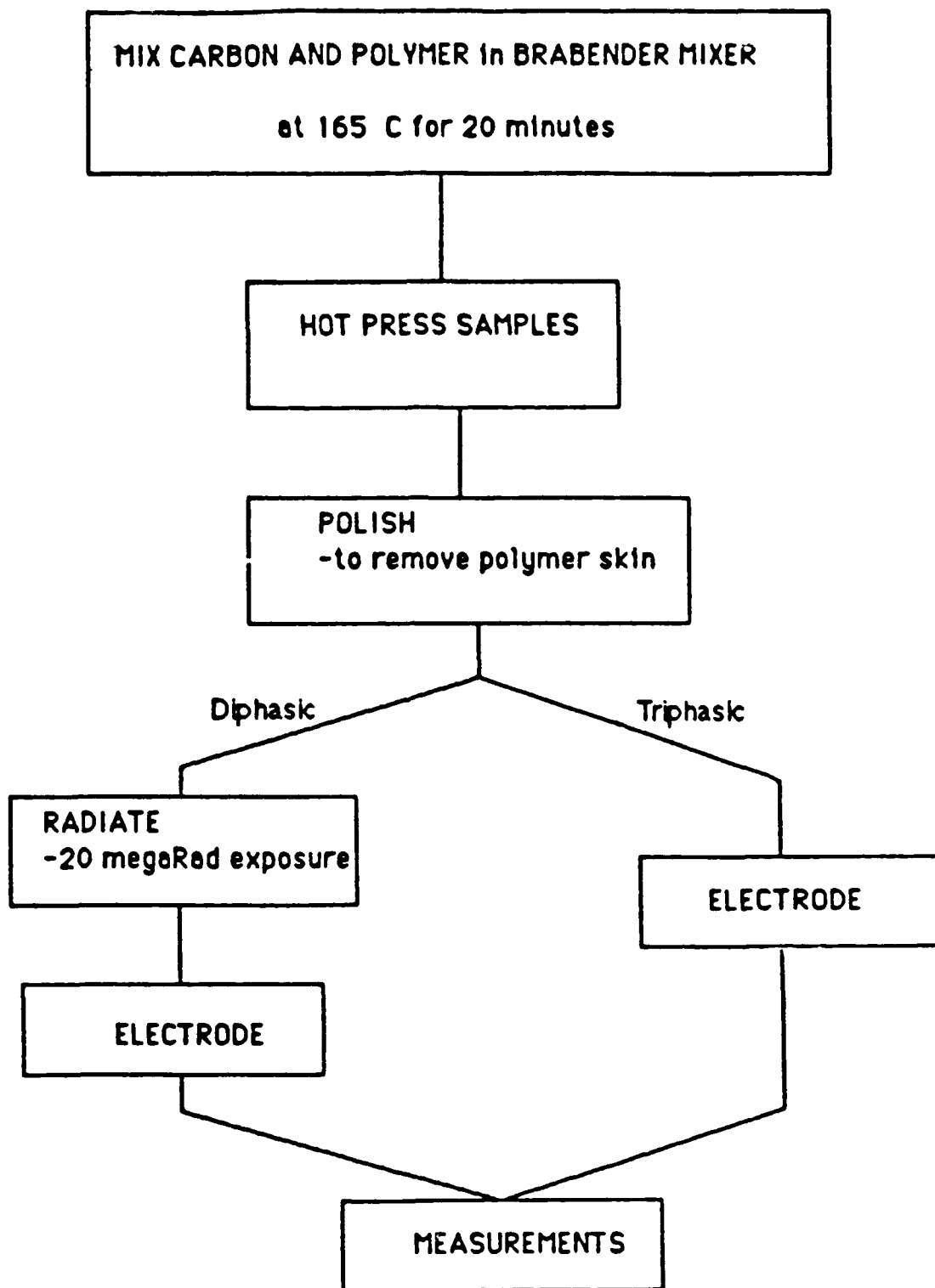
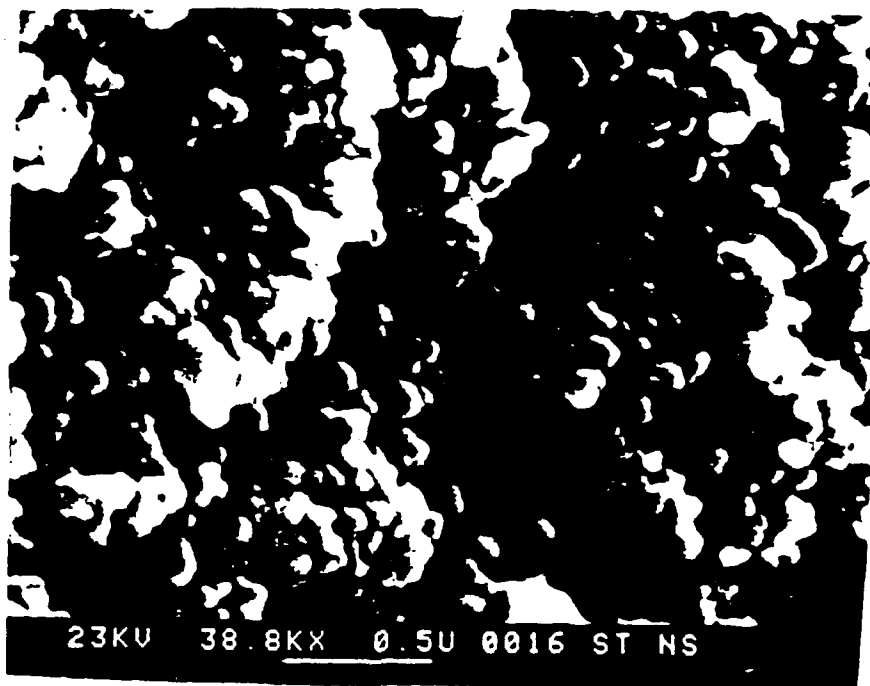


Figure 2.1.1 Outline of Sample Preparation.

(a)



(b)

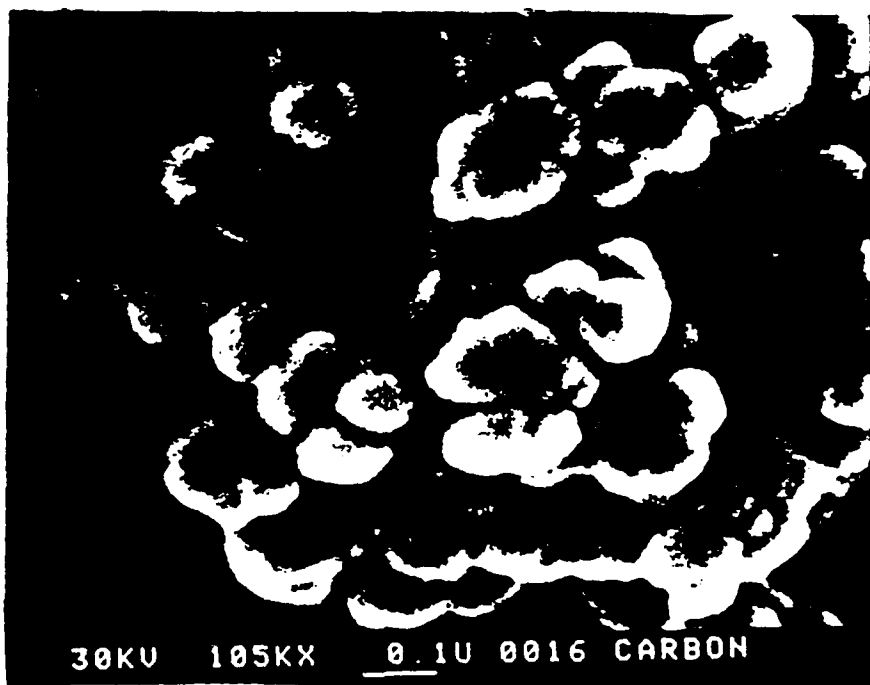


Figure 2.1.2 Scanning Electron Micrographs of Carbon Black.

Table 2.1.1 Particle Characteristics of Starting Powders

	Company	Particle Shape	Avg. Diameter ( $\mu\text{m}$ )
Carbon Black Sterlings NS	Cabot	spherical	0.075
Mullite Zeospheres 200	Zeelan	spherical	1.3
$\alpha$ -Alumina A-14	ALCOA	tabular	4.0
$\alpha$ -Alumina AKP-30	Sumitoma	equiaxed	0.42

employed mullite ( $\text{Al}_2\text{O}_3\text{-SiO}_2$ ) Zeospheres 200 (Zeelan Inc.) as the insulating phase. Zeospheres are very strong, hard, inert spheres used as a processing aid in the production of polymer products.<sup>(34)</sup> Scanning electron micrographs (Figure 2.1.3) show the very spherical shape and the somewhat broad particle size distribution. The average particle size, determined by a Coulter Counter (Coulter Electronics), was determined to be 1.3  $\mu\text{m}$ .

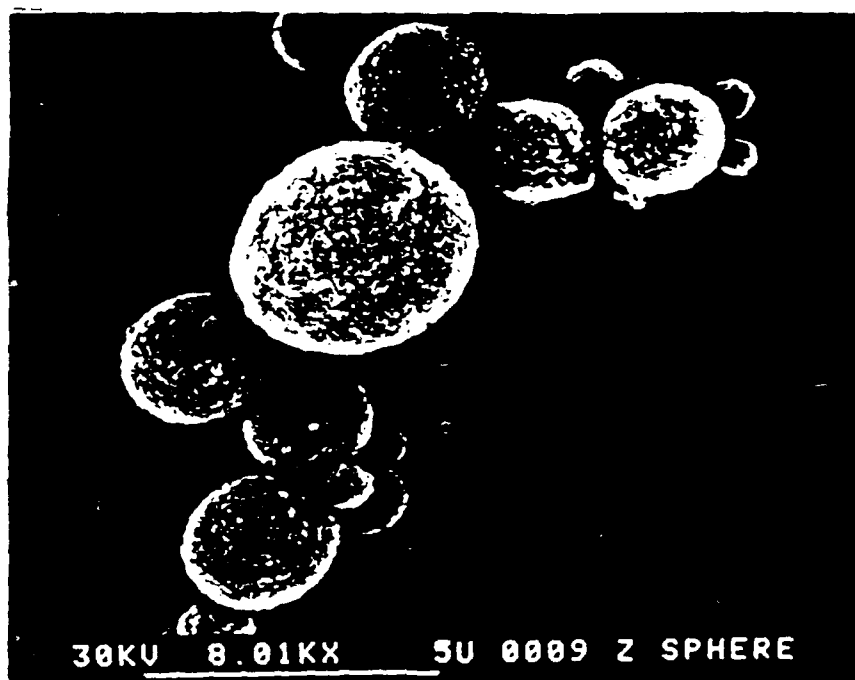
The other two insulating powders used, A-14  $\text{Al}_2\text{O}_3$  (Alcoa) and AKP-30  $\text{Al}_2\text{O}_3$  (Sumatoma Co.) are shown in scanning electron micrographs in Figure 2.1.4. The A-14 is comprised of tabular particles with an average particle diameter of 4.0  $\mu\text{m}$ . The AKP-30 particles appear equiaxed and much smaller, with an average particle size of 0.42  $\mu\text{m}$ .

## 2.2 SAMPLE PREPARATION

The carbon black-polyethylene composites were prepared according to the procedure outlined in Figure 2.1.1. Compositions of interest ranged from 5 to 40 volume percent carbon black. The batch calculations were based on the theoretical density of carbon black.

The carbon black powder and the polyethylene beads are weighed out to  $\pm 0.001$  grams. The actual mixing of the two components occurs in a Brabender mixer (C.W.Brabender Inc.) equipped with an automatic temperature controller

(a)



(b)



Figure 2.1.3 Scanning Electron Micrographs of Mullite Zeospheres.

(a)



(b)

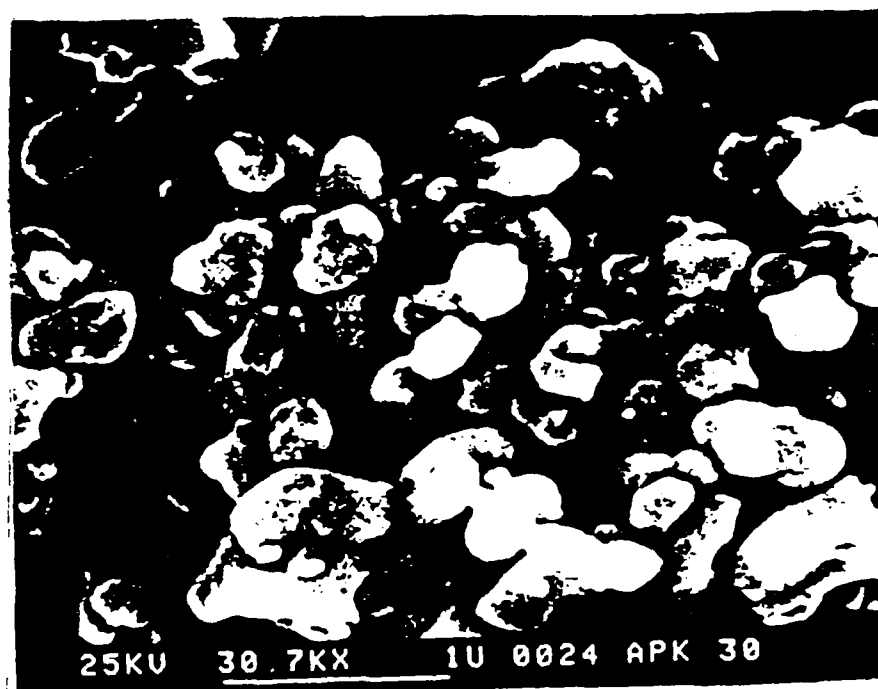


Figure 2.1.4 Scanning Electron Micrographs of (a) A-14 Alumina and (b) AKP-30 Alumina Powders.

(C.W.Brabender Inc.). The Brabender is simply a high temperature shear mixer that permits mixing of the carbon black into the molten polymer.

The Brabender is first heated to 165°C, well above the melting temperature of polyethylene (130°C). This temperature is needed to obtain a low polymer viscosity to insure proper mixing. The polyethylene beads are then added to the mixing chamber and allowed to melt while the shear rate is maintained at 10 R.P.M.. After the polymer has melted, the carbon black is added gradually. The shear rate is then increased to 40 R.P.M. and the two components allowed to mix for 20 minutes. Longer mixing times may lead to polymer degradation and increased difficulty in removing the material from the Brabender. The composite mixture is removed from the mixing chamber while it is still hot and pliable. This permits the composite mixture to be easily broken up into small pieces.

Next, the composite mixture is formed into disc-shaped samples by hot pressing. Approximately 2 grams of the carbon-polyethylene mixture are placed into a one inch diameter steel die. The die is then placed onto a uniaxial Carver Hydraulic Press equipped with an accompanying Carver hot plate. The hot press and die are then heated together with no pressure applied. When the hot plate temperature reaches approximately 180°C, 12,700 psi ( $8.76 \times 10^7$  N/m<sup>2</sup>) of pressure is applied to the die. If too high a pressure is applied, the composite material will extrude out of the die.

The die is held at this temperature and pressure for 20 minutes, to allow the material to flow into the desired shape. Insufficient heat or time will result in porosity in the samples. After 20 minutes, the hot plate is turned off. The die remains under full pressure for at least an hour while cooling to prevent the sample from deforming while the polymer is still soft. After an hour, the die is removed from the press and allowed to finish cooling to room temperature before the sample is removed. The dies must be completely cooled before sample is removed to prevent scoring of the die and sample. The samples produced are one inch diameter discs with a thickness of 2-4 mm, depending on the amount of material used and the amount of flashing that occurs.

The rough edges are removed by polishing the samples with 200 grit followed by 400 grit SiC polishing paper. More importantly, polishing removes the thin polymer skin that forms on the surfaces of the samples during hot pressing. This skin, when not removed, acts as two high resistivity layers on both top and bottom surfaces of the sample, resulting in much larger and much less reproducible resistivity measurements.

The samples are now ready to be crosslinked. Crosslinking of the samples was carried out at the Pennsylvania State University Brezeale Nuclear Reactor under the supervision of Mr. Joseph Bonner. Crosslinking was induced by exposure to a high energy gamma radiation source.

The samples received 90 hours of exposure time to a gamma source that emits 222 KRads/hr for a total dose of 20 MegaRads. (20 Megarads was the dosage listed in the Raychem patents)<sup>(20, 21)</sup>. It proved to be crucial to the reproducibility characteristics of the composite that the 90 hours of exposure be continuous, not intermittent.

Lastly, the electrodes were applied to the sample. Throughout this study, air dry silver paste was used as the electrode material. Gold sputtering and aluminum evaporation methods were unsuitable because the heat generated by these processes caused damage to the polymer surfaces and resulted in inadequate electrical contacts.

The procedure for making the triphasic composites is virtually the same as for the diphasic composites except for the crosslinking step. The triphasic composites are not irradiated and therefore remain uncrosslinked. Also, the mixing temperature of the Brabender is increased from 165°C to 180°C and the hot press temperature is raised to 200°C when a third constituent is present in a composite. Measurement techniques for both the diphasic and the triphasic samples are the same.

### 2.3 COMPOSITE CHARACTERIZATION

The geometric densities of both the diphasic and the triphasic composites were measured and compared to

theoretical densities. Density measurements were used as a tool to check for the presence of porosity within the samples. Scanning electron micrographs were used to determine the degree of mixing in the composites.

Table 2.3.1 lists the densities of the diphasic samples, both crosslinked and uncrosslinked. No change in density was observed when the samples were crosslinked. One trend that was observed was the increased deviation from theoretical density as the carbon black concentration was increased. The deviation from theoretical density is caused by the high degree of porosity and interfloc pores found in carbon blacks. Therefore, the actual density of carbon black is lower than the theoretical density value used in the calculation of theoretical composite densities. Increasing the concentration of carbon black increases the error in the theoretical composite densities. Back calculating the density of carbon black from the measured density yields an apparent density of approximately 2.00 grams/cm<sup>3</sup>. Recalculated theoretical densities using 2.00 grams/cm<sup>3</sup> are listed in Table 2.3.2. The measured densities agree much better with the recalculated theoretical densities.

Table 2.3.3 lists the densities for the triphasic composites. The triphasic samples show the same increase in the deviation from theoretical density as the concentration of carbon black is increased. Comparison of the measured density to the theoretical density calculated using 2.00

Table 2.3.1 Comparison of Geometric and Theoretical Densities for Diphasic Samples

Composition (C-PE)	$\rho_{theo.}$ (g/cm <sup>3</sup> )	$\rho_{geom.}$ (g/cm <sup>3</sup> )	$\Delta\rho(\%)$
10-90	1.09	1.06	2.2
15-85	1.16	1.11	4.5
20-80	1.22	1.15	6.1
25-75	1.27	1.19	6.7
30-70	1.35	1.23	9.8
35-65	1.41	1.29	9.3
40-60	1.48	1.34	9.6

Table 2.3.2 Comparison of Geometric and Re-calculated Theoretical Densities for Diphasic Samples

Composition (C-PE)	$\rho_{theo.}^*$ (g/cm <sup>3</sup> )	$\rho_{geom.}$ (g/cm <sup>3</sup> )	$\Delta\rho(\%)$
10-90	1.07	1.06	0.8
15-85	1.12	1.11	0.9
20-80	1.17	1.15	1.9
25-75	1.22	1.19	2.5
30-70	1.28	1.23	3.7
35-65	1.33	1.29	2.9
40-60	1.38	1.34	3.0

\* calculated using 2.0 g/cm<sup>3</sup> as density of carbon black

Table 2.3.3 Comparison of Theoretical and Geometric Densities of Triphasic Samples

Composition	$\rho_{theo.}$ (g/cm <sup>3</sup> )	$\rho_{geom.}$ (g/cm <sup>3</sup> )	$\Delta\rho(\%)$
10-50-40	1.77	1.73	2.3
10-60-30	1.89	1.85	2.2
15-30-55	1.56	1.50	4.0
15-40-45	1.69	1.63	3.7
15-50-35	1.82	1.77	2.8
20-25-55	1.56	1.45	7.6
20-30-50	1.62	1.53	5.9
20-35-45	1.69	1.59	6.3
20-40-40	1.76	1.65	6.1
20-45-35	1.82	1.72	5.8
20-50-30	1.89	1.81	4.4
25-20-55	1.55	1.44	7.6
25-25-50	1.62	1.54	5.2
25-30-45	1.69	1.57	7.6
25-35-40	1.75	1.62	8.0
25-40-35	1.82	1.69	7.7
30-30-40	1.75	1.63	7.4

grams/cm<sup>3</sup> as the density of carbon black appears in Table 2.3.4. The geometric densities of the triphasic composites also show better agreement with the recalculated theoretical densities.

Scanning electron micrographs of a diphasic 40-60 [40 volume % carbon black-60 volume % PE] sample appear in Figure 2.3.1. The very small size and low atomic number of the carbon black renders it very difficult to distinguish carbon black particles from the polymer matrix, even at high carbon black concentrations.

Scanning electron micrographs of a triphasic 20-50-30 [20 volume% carbon black- 50 volume% mullite- 30 volume% PE] sample appear in Figure 2.3.2. The large mullite spheres are well dispersed throughout the matrix. This confirms that the triphasic composites are thoroughly mixed in the Brabender and that the insulator phase stays well dispersed during subsequent sample preparation.

#### 2.4 ELECTRICAL RESISTANCE MEASUREMENTS

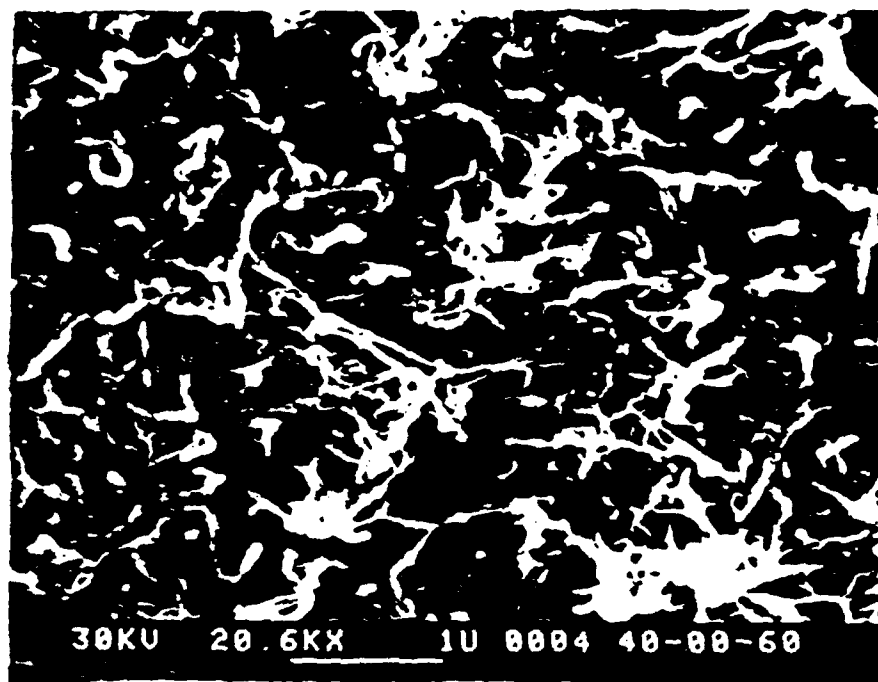
The room temperature resistance of the samples at a frequency of 1 KHz was measured to  $\pm 0.005 \Omega$  on a Hewlett-Packard (HP) 4274A Automatic LCR Bridge. Resistance measurements were also taken at 100 Hz, 10 KHz, 100 KHz, and 1 MHz, but no frequency dispersion occurred at room temperature. The resistivity was calculated using the

Table 2.3.4 Comparison of Geometric and Re-calculated Theoretical Densities of Triphasic Samples

Composition	$\rho_{\text{geo.}}^*$ (g/cm <sup>3</sup> )	$\rho_{\text{geom.}}$ (g/cm <sup>3</sup> )	$\Delta\rho(\%)$
10-50-40	1.74	1.73	1.1
10-60-30	1.87	1.85	1.1
15-30-55	1.52	1.50	1.3
15-40-45	1.65	1.63	1.2
15-50-35	1.79	1.77	1.1
20-25-55	1.51	1.45	4.1
20-30-50	1.57	1.53	2.6
20-35-45	1.64	1.59	3.1
20-40-40	1.71	1.65	3.6
20-45-35	1.77	1.72	2.9
20-50-30	1.84	1.81	1.7
25-20-55	1.49	1.44	3.4
25-25-50	1.56	1.54	1.3
25-30-45	1.62	1.57	3.2
25-35-40	1.69	1.62	4.3
25-40-35	1.76	1.69	4.1
30-30-40	1.68	1.63	3.1

\* calculated using 2.0 g/cm<sup>3</sup> as density of carbon black

(a)

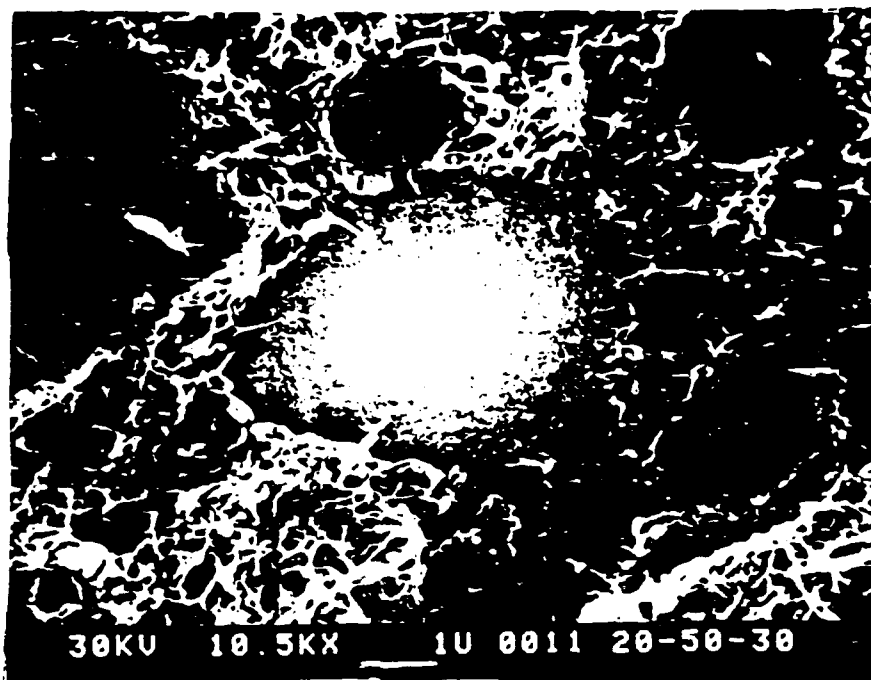


(b)



Figure 2.3.1 Scanning Electron Micrographs of a Diphasic Composite.

(a)



(b)

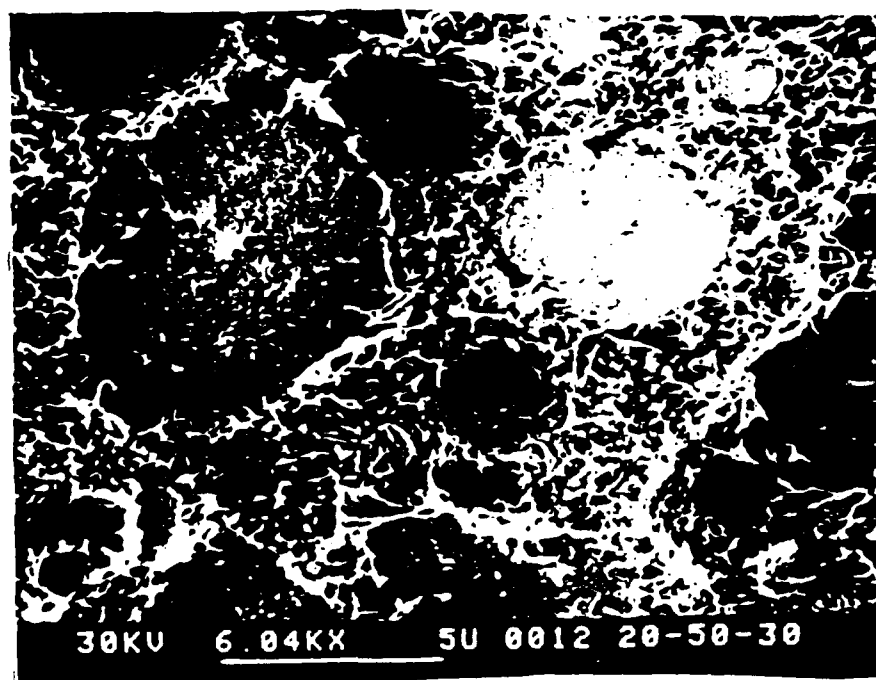


Figure 2.3.2 Scanning Electron Micrographs of a Triphasic Composite.

relation:

$$\rho = R A / t$$

where R is the measured resistance, A is the area of the sample and t is the thickness. When resistivity was plotted as a function of composition, the resistivity value at a given composition is the median value of 4 to 6 samples.

Resistance was measured as a function of temperature between 25°C and 200°C. The resistance was measured with an HP 4274A and HP4275A digital LCR Bridges interfaced to an HP 9816 computer by an HP 6940B Multiprogrammer and an HP 59500A Multiprogrammer Interface. One volt was applied to a sample. The resistance of the sample was determined by the corresponding current and digitally displayed to +/- 0.001Ω on the LCR Bridge. Measurements were made at frequencies ranging from 100 Hz to 1 MHz.

The temperature was controlled in a Delta Design 2300 electrical resistance box furnace interfaced to the HP 9816 computer. Using software provided by P. Moses, the HP 9816 computer controlled the rate of heating and cooling by regulating the flow of liquid nitrogen into the furnace. Heating and cooling rates between 1°C/min and 4°C/min were tested. Varying the rate had no effect on the final results, so 4°C/min was used throughout this study. Resistivity was automatically calculated from the measured resistance when the data was plotted.

To determine their reproducibility on thermal cycling, the samples were subjected to multiple heating and cooling cycles using the apparatus just described. The multiple cycles were performed consecutively. This led to contact problems caused by the condensation of water onto the samples during a heating run that was preceded by a cooling run. To eliminate this problem, the samples were held at room temperature for ten minutes at the completion of each cooling cycle, during which time any condensed water was dried off by a flow of warm air.

To determine the recovery time of the samples, room temperature resistance measurements were taken prior to any thermal cycling. This is the initial or base resistance of the samples. The samples were then heated to 160°C and cooled back to room temperature. The resistance of the sample was measured again and compared to the initial value. Sample resistance was measured again after 24 hours. Subsequent heating and cooling cycles were tested in the same manner.

## 2.5 HIGH POWER TESTING

Some of the composite samples were sent to Dr. Manfred Kahn at the Naval Research Laboratory for high power testing. The maximum steady state voltage the samples can withstand, as well as the pulse current and voltage

characteristics are determined. The mechanisms of high power breakdown are studied.

## CHAPTER THREE

## RESISTIVITY MEASUREMENTS - PERCOLATION

Resistance measurements were made on all of the diphasic carbon black-polyethylene (PE) and the triphasic carbon black-insulator-PE composite systems. The composite samples were prepared according to the procedure outlined in section 2.2. The measurement techniques are described in section 2.4.

Sterlings N.S. carbon black was used throughout this study to eliminate the variables associated with different carbon blacks, such as particle size and distribution, morphology, degree of agglomeration and dispersibility. A large fraction of the triphasic composites contained mullite Zeospheres as the insulating filler. Diligent efforts were made to insure that the sole variable was the one under study.

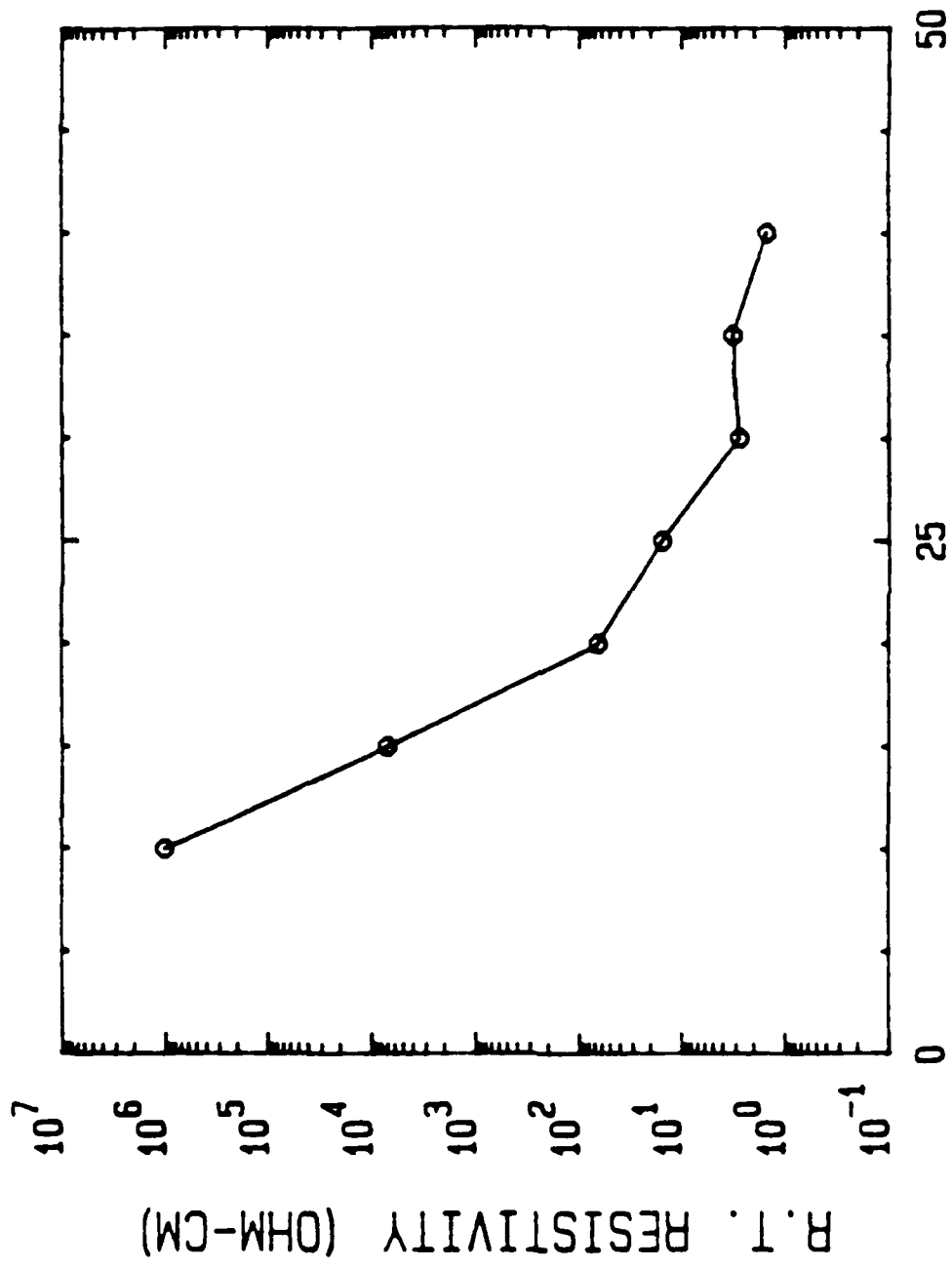
Resistance measurements were taken at 100 Hz, 1 KHz, 10 KHz, 100 KHz, and 1 MHz. All room temperature resistances shown were taken at 10 KHz. There was no frequency dispersion in the room temperature resistivity. All resistance measurements were converted to resistivity to eliminate the effects of sample size.

### 3.1 PERCOLATION IN DIPHASIC COMPOSITES

The percolation phenomenon in carbon black loaded PE has been well documented.<sup>(2,3,7-11)</sup> The shape and location of the curve is very dependent on the type of carbon black used. Finer sized carbon blacks give lower percolation threshold concentrations than larger sized carbon blacks.<sup>(3)</sup> The steepness of the percolation curve is dependent on the "structuredness" of the carbon black. More highly structured blacks result in steeper percolation curves than less structured blacks.<sup>(3)</sup>

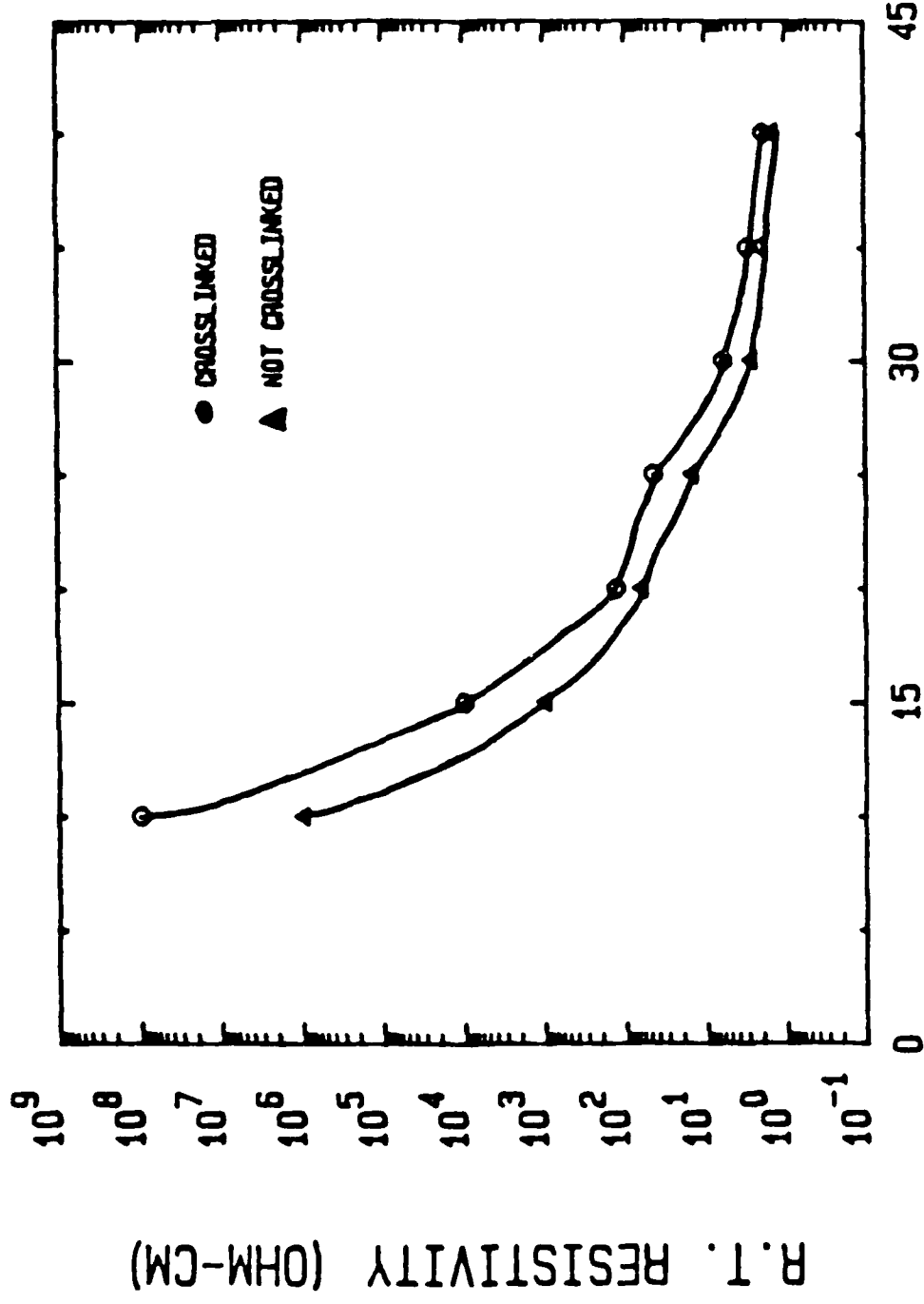
Figure 3.1.1 is a plot of room temperature resistivity as a function of carbon black concentration for a carbon black loaded PE that has not been crosslinked. This percolation curve is somewhat broad, indicative of the low degree of structure found in Sterlings NS.<sup>(36,37)</sup> Because of the large particle size of Sterlings NS, the percolation threshold concentration, approximately 10 volume % carbon black, is slightly higher than it would be if a smaller particle size carbon black were used.

Figure 3.1.2 illustrates the effects of radiation induced crosslinking on the resistivity of a carbon black-PE composite. A slight increase in resistivity occurs after the samples are crosslinked. This is consistent with results published by Narkis.<sup>(27)</sup> Narkis also observed a



VOLUME % CARBON BLACK

Figure 3.1.1 Percolation Curve for Uncrosslinked Composites.



### VOLUME PERCENT CARBON BLACK

Figure 3.1.2 Comparison of Crosslinked and Uncrosslinked Percolation Curves.

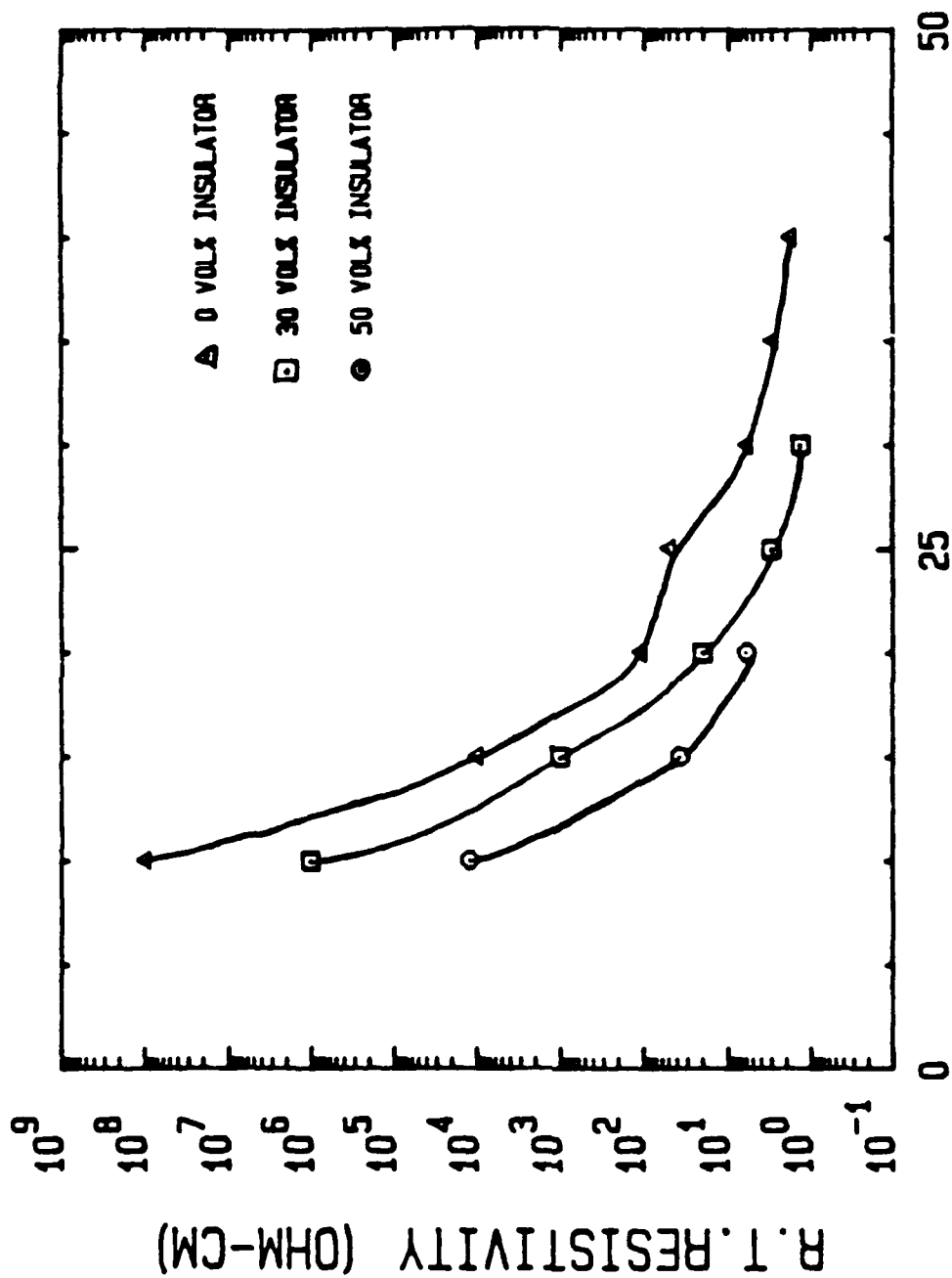
strong attachment of the carbon black particles to the PE network only after crosslinking. This attachment could be causing a minute separation of the carbon black particles, accounting for the slight increase in resistivity.

### 3.2 PERCOLATION IN TRIPHASIC COMPOSITES

When an insulating filler is incorporated into the carbon black-PE mixture to form a triphasic composite, the percolation curve is expected to shift to the right, or toward higher resistivities.<sup>(38)</sup> However, upon addition of an insulating mullite phase the percolation curve shifted to the left, or toward lower resistivities. This is shown in Figure 3.2.1. The more mullite that is added, the farther left the curve shifts. This means that for a given carbon black concentration, adding an insulating phase will decrease the resistivity, not increase it.

When the mullite Zeospheres were added to a  $V_2O_5$ -PE composite mixture, the percolation curve shown in Figure 3.2.2 shifted to the right. Therefore at a given concentration of  $V_2O_5$ , adding an insulator increased the resistivity, the opposite trend from that seen in the carbon black-Zeosphere-PE system.

The reason for different behavior between the three phase carbon black system and the three phase  $V_2O_5$  system



### VOLUME % CARBON BLACK

Figure 3.2.1 Percolation Curve for Triphasic Carbon Black Composites.

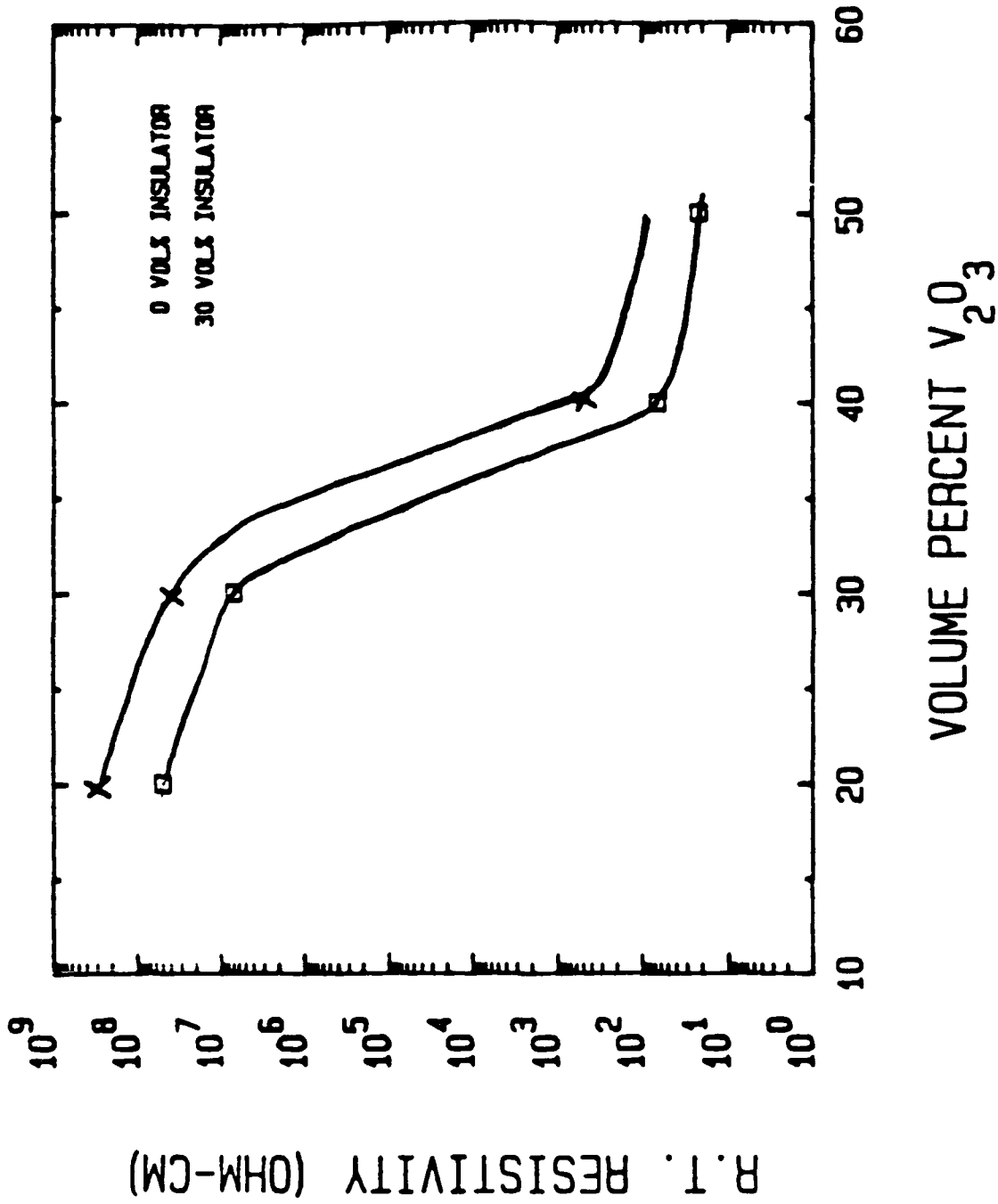


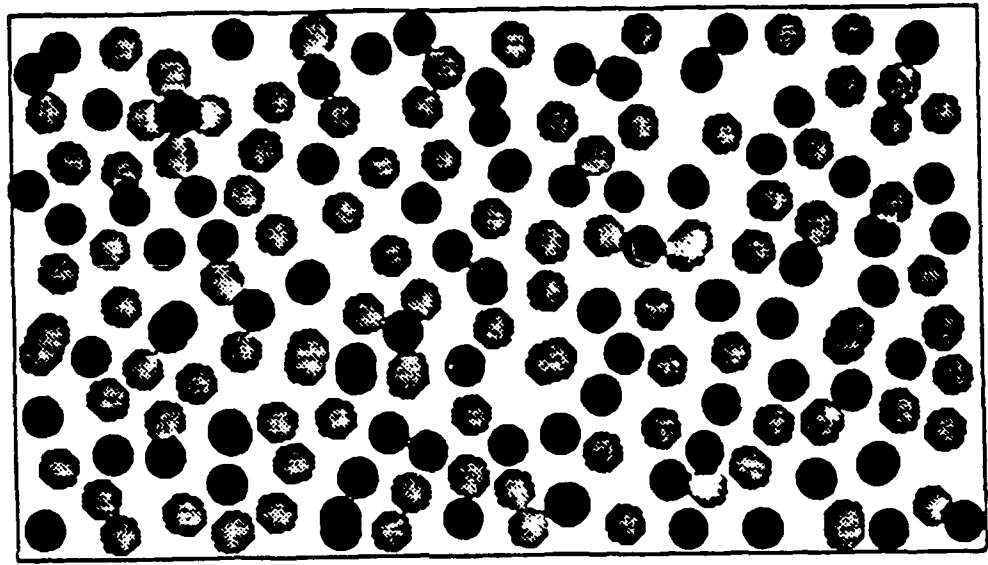
Figure 3.2.2 Percolation Curve for Triphasic V O 2 3 Composites.

can be related to the size differential between the conductor particles and the insulator particles. The  $V_2O_5$  particles (average diameter=4.0  $\mu\text{m}$ ) and the Zeospheres (average diameter=1.3  $\mu\text{m}$ ) are approximately the same size, so they form a simple 0-0-3 type of connectivity, illustrated in Figure 3.2.3a. The carbon black particles (average diameter=0.075  $\mu\text{m}$ ) and the Zeospheres are two orders of magnitude different in size. This size differential leads to the formation of a quasi-composite phase.<sup>(6)</sup> The carbon black-Zeospheres-PE system forms a 3(0-3)-0 type of connectivity, as seen in Figure 3.2.3b. The carbon black and PE form a quasi-phase with 0-3 connectivity. This quasi-phase in turn is three dimensionally connected throughout the composite, and the Zeospheres are zero-connected.

These different connectivities may be used to rationalize the different trends of the two systems. When Zeospheres are added to the  $V_2O_5$  and PE mixture, they interfere with the conduction chains or paths, causing an increase in the resistivity of the composite. The more Zeospheres that are present, the more conduction paths will be interrupted. Interrupted paths correspond to increased resistivity.

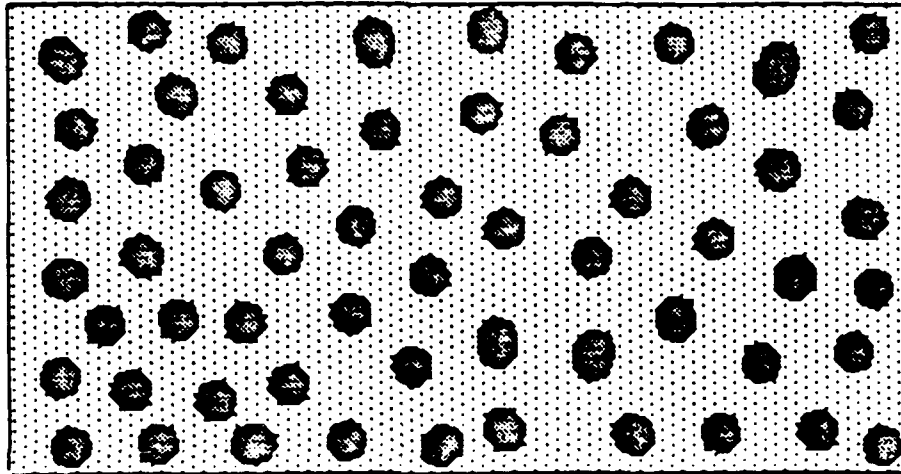
When Zeospheres are added to the carbon black-PE mixture, the resistivity decreases. This occurs because the Zeospheres are much larger than the carbon black particles. The Zeospheres restrict the carbon black particles to a

0-0-3



- CONDUCTOR PARTICLE
- ◐ INSULATOR PARTICLE

Figure 3.2.3(a) Schematic of a 0-0-3 Composite Connectivity.

$3(0-3)-0$ 

CARBON BLACK / POLYETHYLENE MIXTURE (0-3)



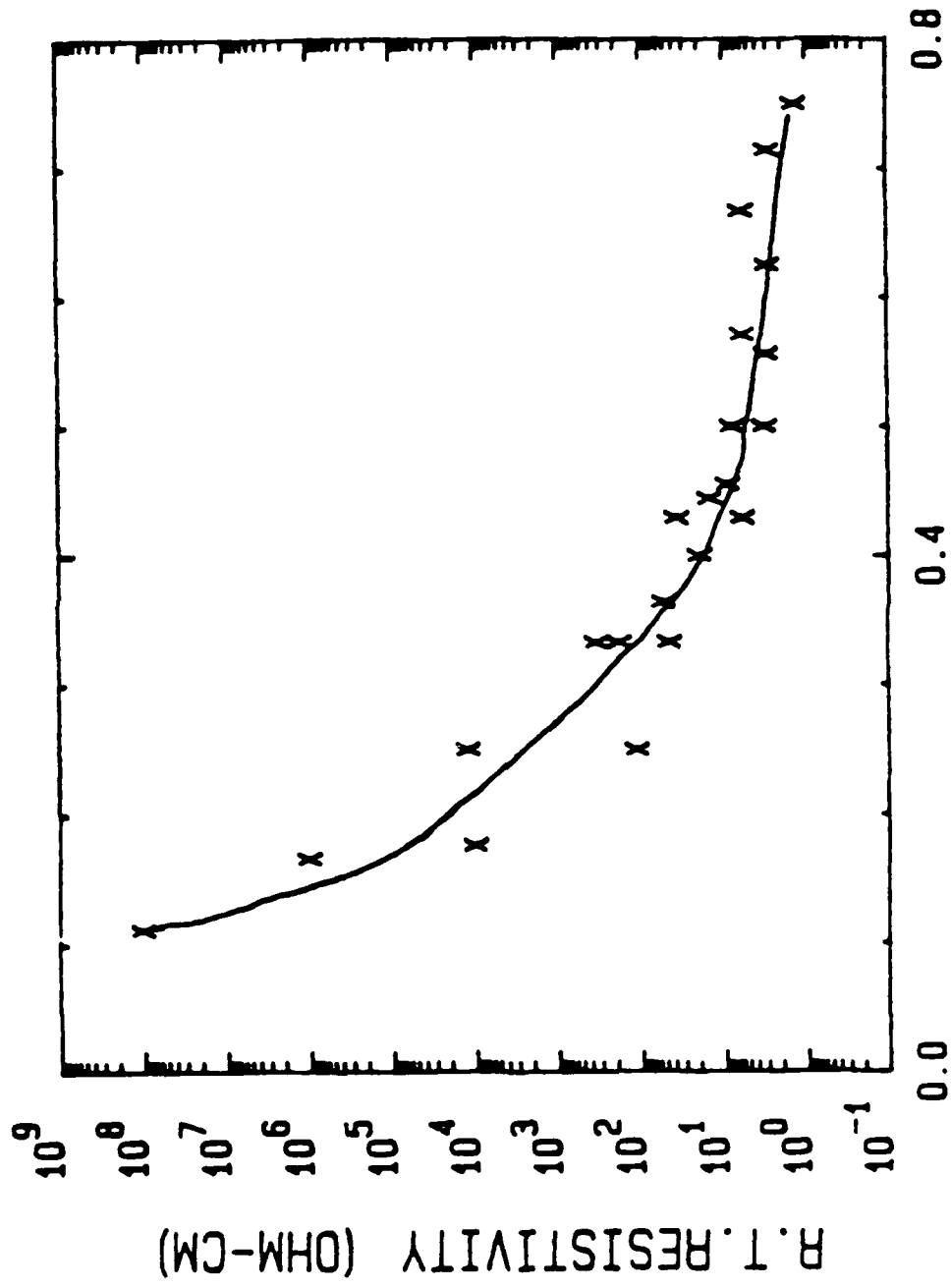
INSULATOR PARTICLES

Figure 3.2.3(b) Schematic of a  $3(0-3)-0$  Composite Connectivity.

smaller volume, consequently forcing them into closer contact with each other. Adding the Zeospheres is equivalent to increasing the carbon black/PE ratio by decreasing the volume of PE. Increasing the carbon black/PE ratio when a 3(0-3)-0 type of connectivity exists will result in a decrease of the composite resistivity, as shown in Figure 3.2.4.

The difference in direction of percolation curve motion can also be explained in terms of site occupancy. In the  $V_2O_5$  system, the Zeospheres occupy conductor ( $V_2O_5$ ) sites. This is why increasing the conductor to PE ratio increases the resistivity in this system. But in the carbon black system, the Zeospheres do not merely occupy conductor sites. Instead they occupy matrix and conductor sites. Since both matrix sites and conductor sites are occupied, the carbon black particles are excluded from some areas of the matrix and are therefore restricted to a smaller volume. This results in a decrease in resistivity because the carbon black particles are in closer contact and thus able to form more conducting networks. This explains the decrease in resistivity with increasing carbon black/PE ratio. The particular type of site an insulator will occupy depends on the size of both the conductor and the insulator.

A very simple model, similar to the modified cubes model developed by Saito and Banno<sup>(39)</sup>, has been developed to predict the effect of a third filler on the resistivity behavior of the 3(0-3)-0 type of composite. A unit cube



CARBON BLACK / PE RATIO

Figure 3.2.4 Effect of Carbon Black/Polyethylene Ratio on the Resistivity of Carbon Black Composites.

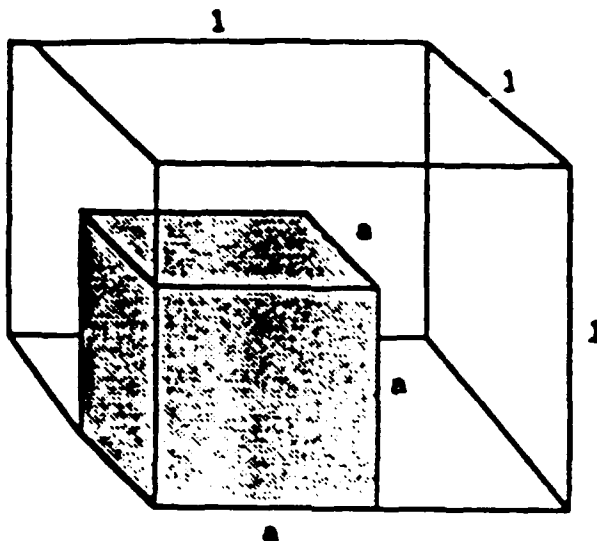
consisting of an insulating cube within a larger cube is used to model the larger scale composite. The volume ratio of the phases within the unit cube are the same as in the overall composite. (Figure 3.2.5)

The total volume of the unit cube sample is  $1 \text{ cm}^3$ . The insulator cube has dimensions "a". The resistivity of the carbon black-PE phase is determined by calculating the volume percent of carbon in the PE and then obtaining the corresponding value of resistivity from the plot of resistivity versus carbon black concentration for diphasic composites. (Figure 3.1.1)

The resistivity of the composite will be a combination of series and parallel conduction models. The series contribution is negligible compared to the parallel contribution. The series contribution is determined first, and then combined with the parallel conductivity model to predict the total resistivity of the composite.

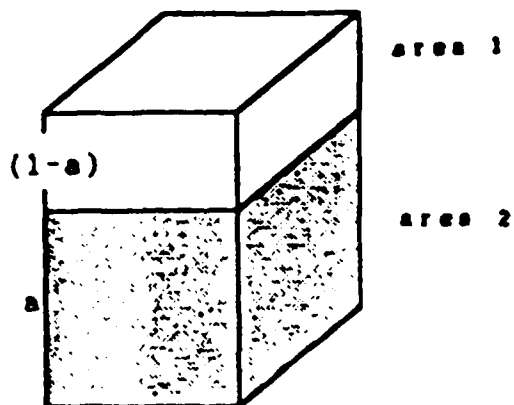
Figure 3.2.6 shows the theoretically calculated shifts in the percolation curve upon addition of an insulating filler which forms a 3(0-3)-0 type of connectivity. The results of the model coincide with the trends seen experimentally. The larger the volume of insulator present in a composite, the more the percolation curve shifts to the left, or toward lower resistivities.

The percolation curve predicted by this model is compared to the actual measured percolation values in Figure 3.2.7. The predictions appear to be more accurate at higher



### SERIES CONTRIBUTION

$$R_{\text{series}} = R_{\text{vol 1}} + R_{\text{vol 2}}$$

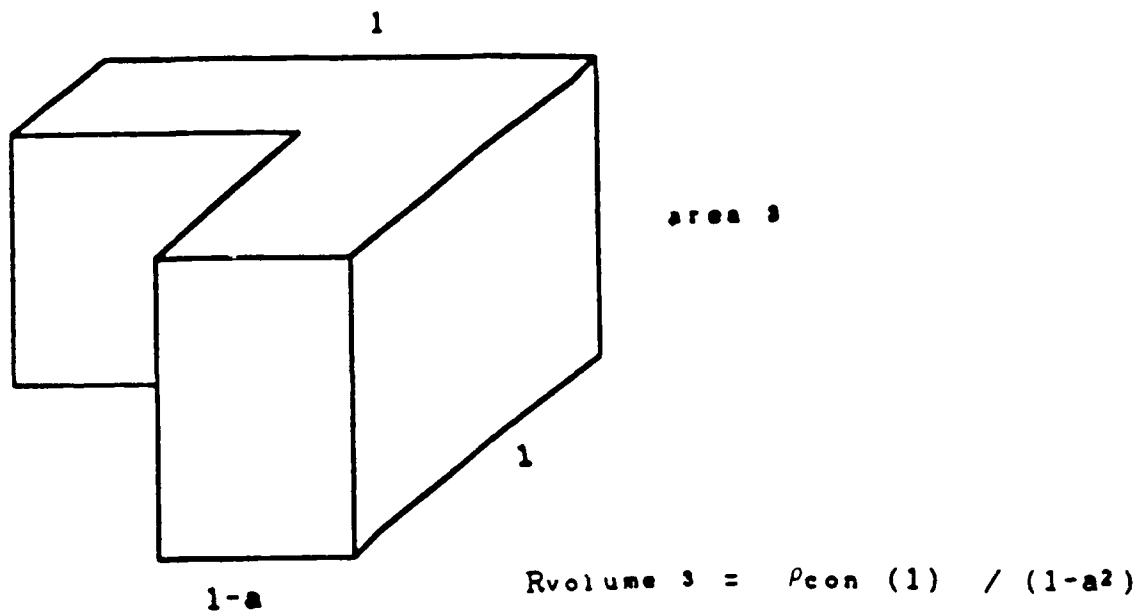


$$R_{\text{volume 1}} = \rho_{\text{con}} (1-a) / a^2$$

$$R_{\text{volume 2}} = \rho_{\text{ins}} (a) / a^2$$

Figure 3.2.5 Model for Theoretical Calculation of Triphasic 3(0-3)-0 Composite Resistivity.

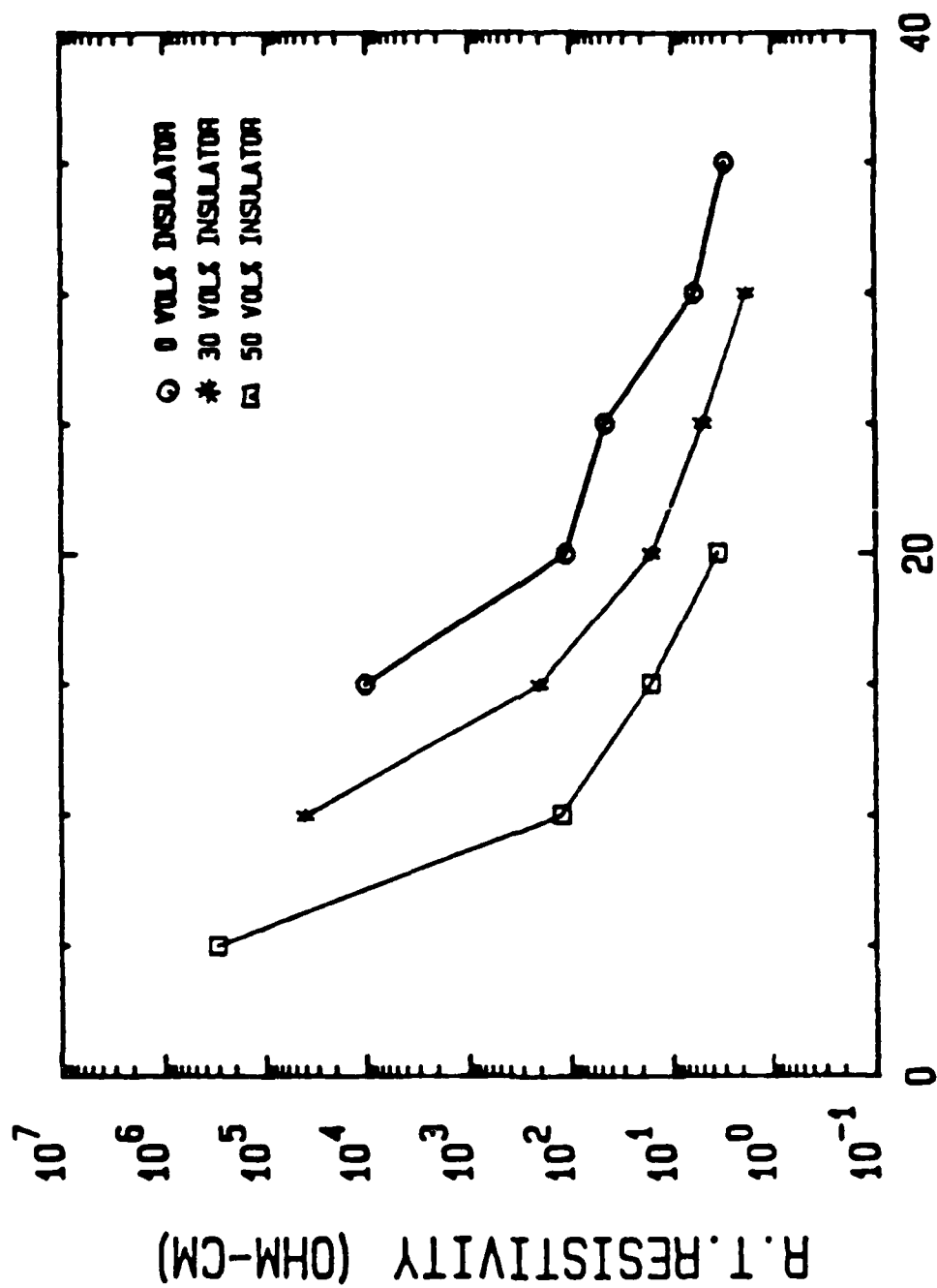
## PARALLEL CONTRIBUTION



$$R_{\text{total}} = \left( \frac{1}{R_{\text{series}}} + \frac{1}{R_{\text{area 3}}} \right)^{-1}$$

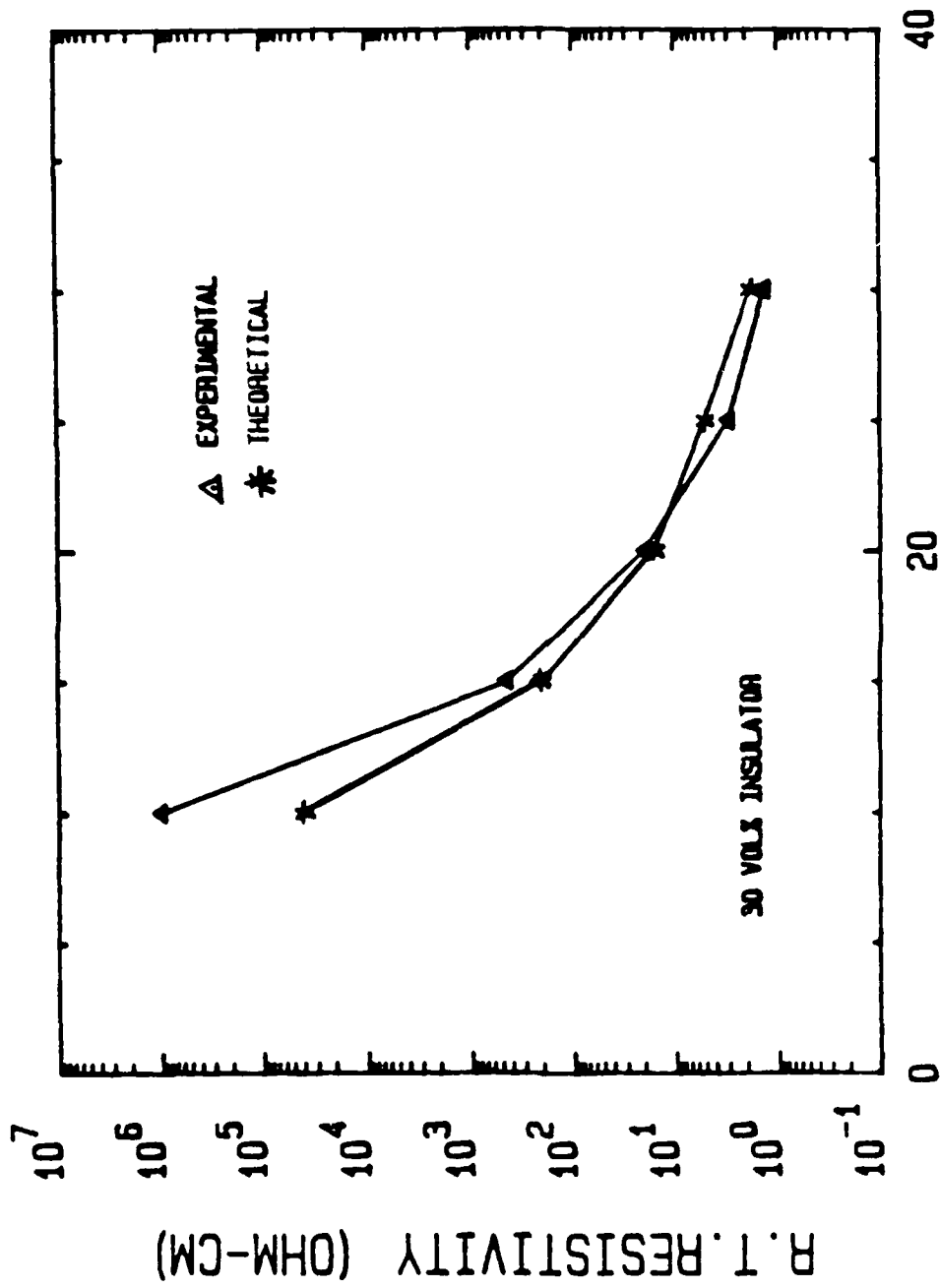
$$R_{\text{total}} = \rho_{\text{total}}$$

Figure 3.2.5 Continued.



### VOLUME % CARBON BLACK

Figure 3.2.6 Theoretical Predictions of Percolation Curves for a 3(0-3)-0 Composite.



### VOLUME % CARBON BLACK

Figure 3.2.7 Comparison of Theoretical and Experimental Percolation Curves for a 3(0-3)-0 Composite.

carbon black concentrations. At lower concentrations of carbon black the model predicts lower resistivities than the composite actually exhibits. One possible explanation for this trend is that the resistivity of the carbon black-PE phase is taken from the resistivity measurements made on diphasic samples. A low volume fraction of carbon black may be slightly more dispersed in the triphasic composites than in the diphasic composites, leading to a higher resistivity of the carbon black-PE phase within the triphasic samples. Evidence of this dispersion effect occurs in the graph of resistivity versus carbon/PE ratio (Figure 3.2.4). At the same carbon black/PE ratio, samples with higher insulator concentrations exhibit slightly higher resistivities.

The 0-0-3 connectivity pattern formed by the triphasic  $V_2O_5$  system follows the model proposed by Zallen<sup>(7)</sup> and others for two different color spheres of the same size, one conducting and one non-conducting. Basically, these models state that a critical number of unblocked sites are needed for conduction to occur. Increasing the insulator concentration increases the number of blocked sites and increases the resistivity.

The relative sizes of the conductor and the insulator appear to be very important in determining the type of connectivity as well as the percolation behavior of a triphasic composite system. This assumption was further tested for the carbon black-insulator-PE system. Two different sized  $Al_2O_3$  powders were substituted for the

Zeospheres (average diameter= 1.3  $\mu\text{m}$ ). The first was an A-14  $\text{Al}_2\text{O}_3$  (Alcoa) with an average particle diameter of 4.0  $\mu\text{m}$  and the second was an AKP-30 (Sumitoma) with an average particle diameter of 0.42  $\mu\text{m}$ .

Figure 3.2.8 illustrates the differences in resistivity for the same compositions produced with each of the three insulators. The same carbon black and PE were used, only the insulator was changed. The samples containing the A-14  $\text{Al}_2\text{O}_3$  showed slightly lower resistivities at a given composition than did those containing Zeospheres. The samples made with the AKP-30  $\text{Al}_2\text{O}_3$  showed substantially higher resistivities than the compositions containing Zeospheres.

The results of the alumina composites are consistent with the idea of quasi-composites proposed in this Section. The A-14  $\text{Al}_2\text{O}_3$  should forms a 3(0-3)-0 type of connectivity. The slightly larger particle size of the A-14  $\text{Al}_2\text{O}_3$  may account for the slightly lower resistivities than those obtained using the Zeospheres. The AKP-30 on the other hand, is much closer in size to the carbon black particles, less than one order of magnitude different. the resistivities of these samples are approximately equal to the resistivities of the diphasic composites containing the same carbon black concentration. The resistivity is only slightly changed by the addition of the AKP-30  $\text{Al}_2\text{O}_3$ . The size difference between the AKP-30 and the carbon black appears to fall on the border between a 3(0-3)-0 and a 0-0-3

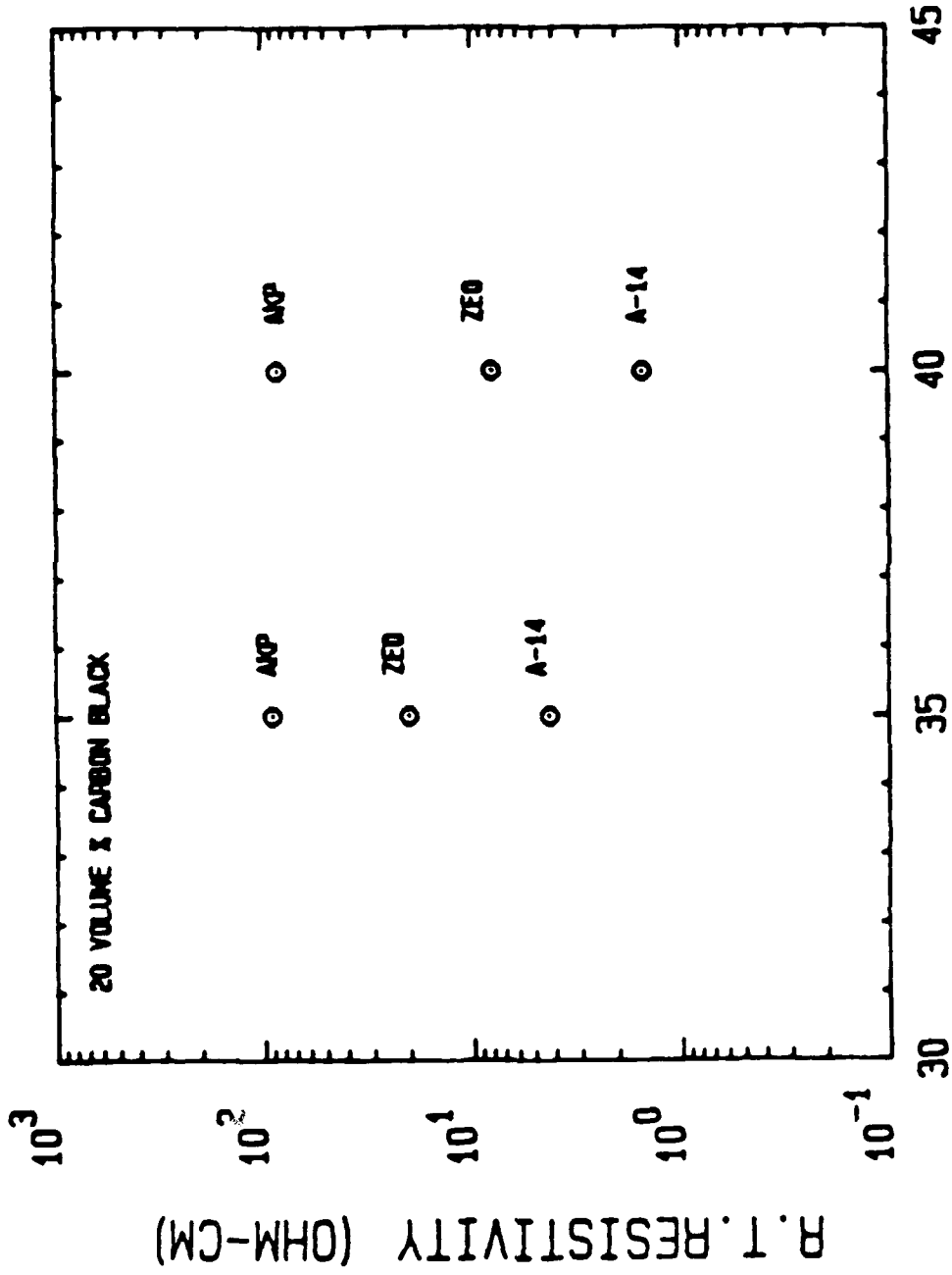


Figure 3.2.8 Effect of Insulator Particle Size on Resistivity of Carbon Black Composites.

type of connectivity pattern, and consequently shows no major effect.

## CHAPTER FOUR

### RESISTIVITY MEASUREMENTS - THE PTC EFFECT

The resistance was measured as a function of temperature from 25-200°C using the apparatus described in Section 2.4. Measurements were taken at frequencies of 1 KHz, 10 KHz, 100 KHz, and 1 MHz. All of the resistivity as a function of temperature graphs are measurements taken at 1 KHz, because at this frequency the greatest PTC effects were observed.

#### 4.1 PTC EFFECT IN DIPHASIC COMPOSITES

The diphasic carbon black-loaded PE composites, when heated to the melting temperature of PE (130°C) exhibit a sharp increase in resistivity known as the PTC effect. The magnitude of the PTC effect depends on the concentration of carbon black. Carbon black concentrations near or slightly above the percolation threshold concentration (in this system approximately 10 volume% carbon black) give the

largest PTC effects. Concentrations well above or below the percolation concentration yield little or no PTC effect.

Figure 4.1.1 illustrates the PTC effect that occurs at several different carbon black-PE compositions that were not crosslinked. These uncrosslinked samples exhibit many undesirable features for a thermistor. First, between room temperature and the PTC transition temperature the resistivity increases considerably. Second, the PTC transition temperature itself is not well defined, but occurs over a broad temperature range. Third, these composites exhibit a substantial NTC effect immediately after the PTC due to the massive rearrangement of carbon black particles. Lastly, uncrosslinked samples above the PTC transition temperature lose mechanical integrity and experience shape deformation or "slumping", rendering the sample useless.

Figure 4.1.2 demonstrates the dramatic effect crosslinking has on the resistivity versus temperature characteristics. After crosslinking, the resistivity remains almost constant below the transition temperature. The PTC transition occurs sharply at a well defined temperature. The transition temperature varies between 125-135°C depending on the amount of filler present in the material. Higher filler concentrations result in higher transition temperatures. For example, 20 volume % carbon switches at 125°C whereas 40 volume % carbon switches at 135°C.

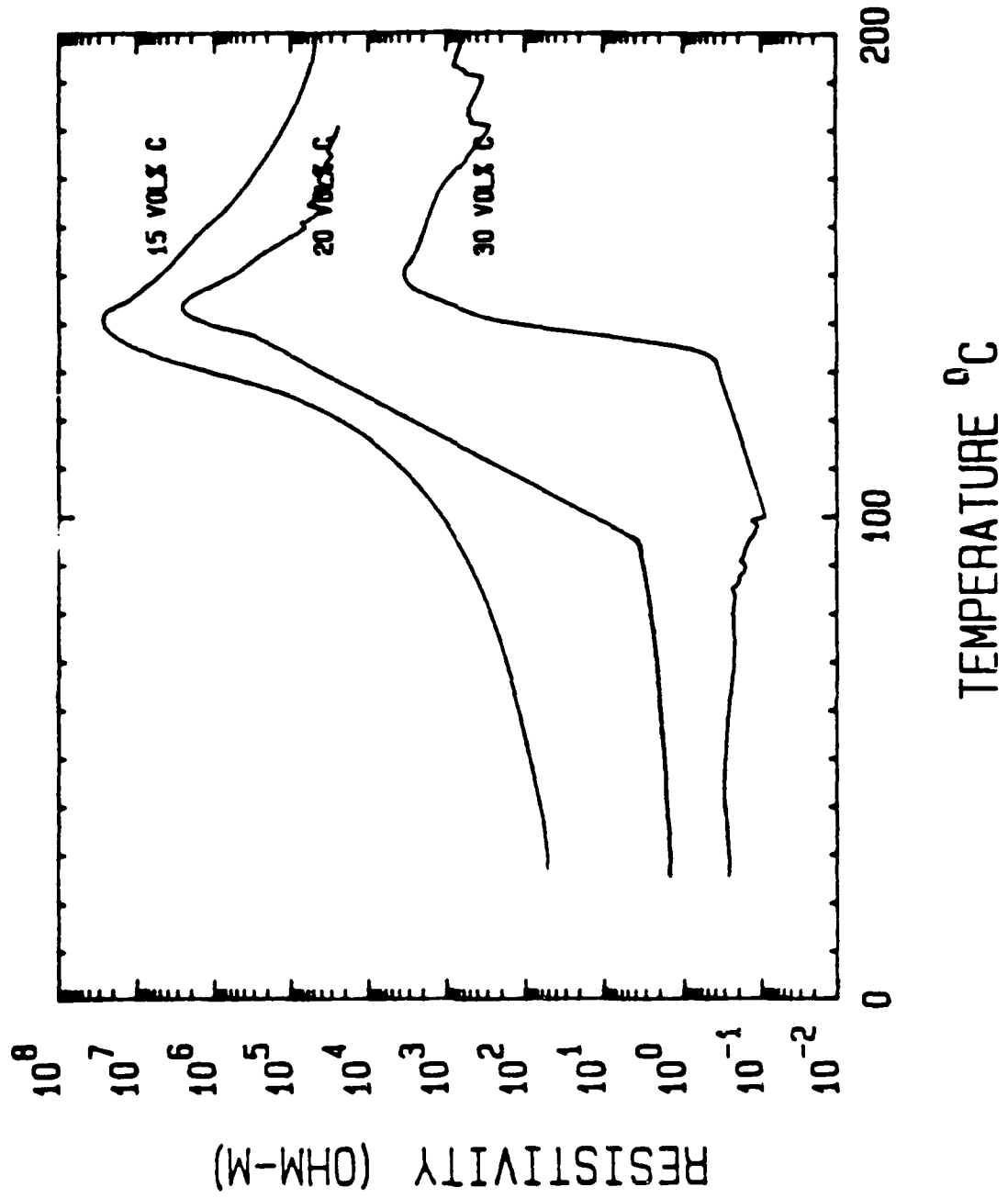


Figure 4.1.1.1 Resistivity-Temperature Curves for Uncrosslinked Composites.

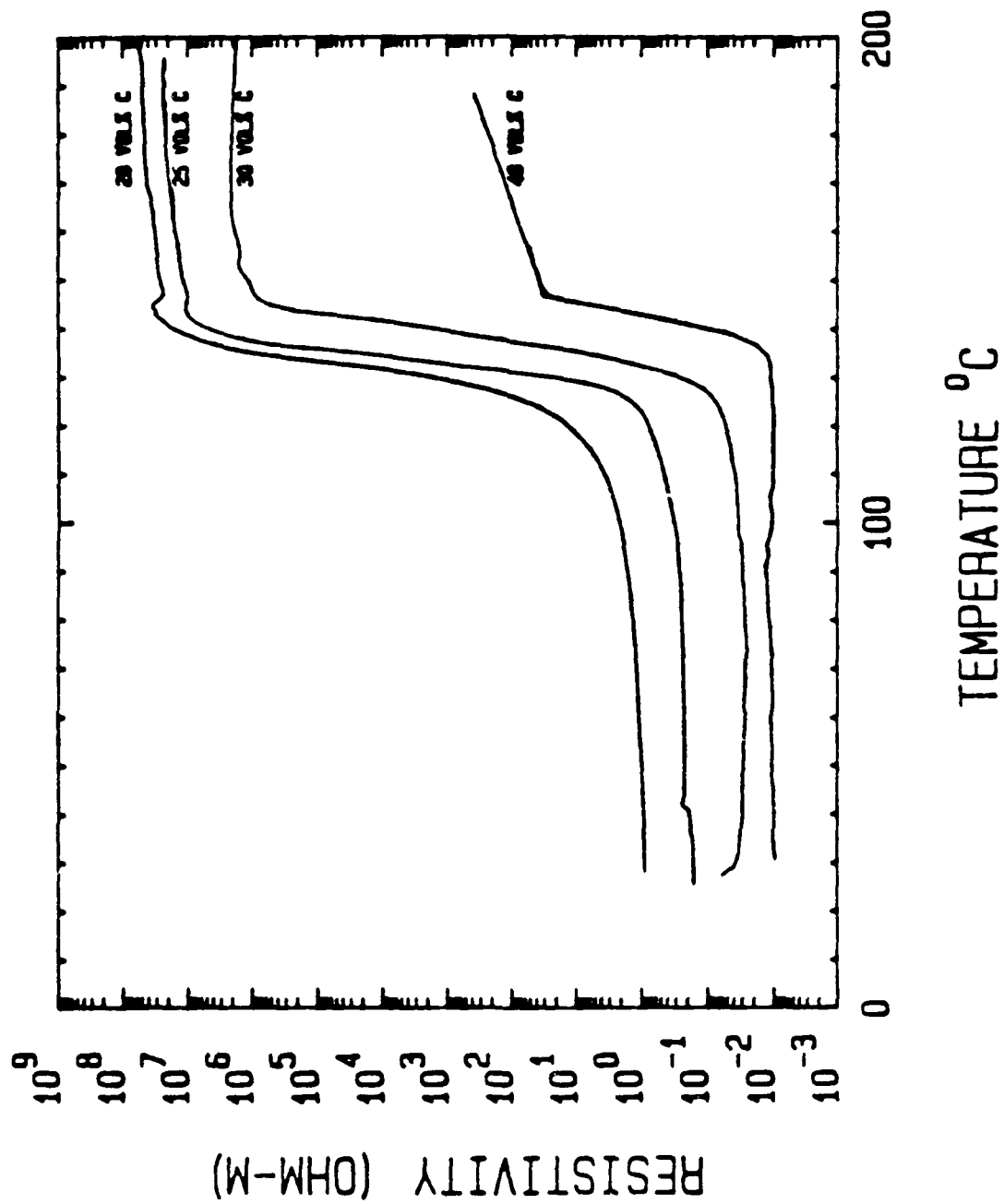


Figure 4.1.1.2 Resistivity-Temperature Curves for Crosslinked Composites.

The key advantages to crosslinking the composites are that it eliminates the NTC and imparts mechanical integrity to the sample at temperatures above the PTC transition temperature. Crosslinking the polymer, as stated in Section 1.5, results in a stabilized polymer network and greatly reduced movement of the carbon black particles. Reduced motion of the carbon black particles prevents sizeable increases in resistivity below the transition temperature. Reduced motion also prohibits the large scale rearrangement of the carbon black particles that causes the NTC above the transition temperature. A stabilized polymer network allows the samples to withstand temperatures substantially above the transition temperature without slumping.

#### 4.2 PTC EFFECT IN TRIPHASIC COMPOSITES

Elimination of the NTC effect at temperatures above the transition temperature is crucial to the practical application of this composite material as a thermistor.<sup>(27)</sup> Thus far, the only satisfactory method of accomplishing this stabilization has been crosslinking. One of the goals of this thesis has been to investigate other methods of producing a suitable thermistor material that does not require crosslinking.

One alternative method explored was to introduce an

insulating third phase into the carbon black-PE mixture in order to stabilize the structure and reduce motion of the carbon black particles without sacrificing the PTC effect. Various amounts of spherical-shaped mullite particles called Zeospheres (average diameter=1.3  $\mu\text{m}$ ) were incorporated into the carbon black-PE mixture. The carbon black concentration was held constant. The concentration of Zeospheres ranged from 0 to 45 volume %.

The resistivity versus temperature characteristics for these triphasic composites are shown in Figure 4.2.1. The 20-0-80 composition corresponds to a diphasic carbon black-PE that was crosslinked. The other compositions correspond to [carbon black]-[insulator]-[PE] that have not been crosslinked. Clearly, the triphasic composites are as good or better than the crosslinked diphasic composite. Not only do the triphasic composites maintain high resistivity and mechanical integrity above the PTC transition temperature, they also exhibit lower room temperature resistivities at a given concentration of carbon black. The greater the concentration of Zeospheres, the more the resistivity versus temperature curve is shifted downward.

There is a limit, however, to how far the curve can be shifted. As seen in Figure 4.2.1, between the 20-40-40 composition and the 20-45-35 composition there is no appreciable decrease in resistivity, but there is a substantial decrease in the magnitude of the PTC effect. The optimum composition in this carbon black-Zeospheres-PE

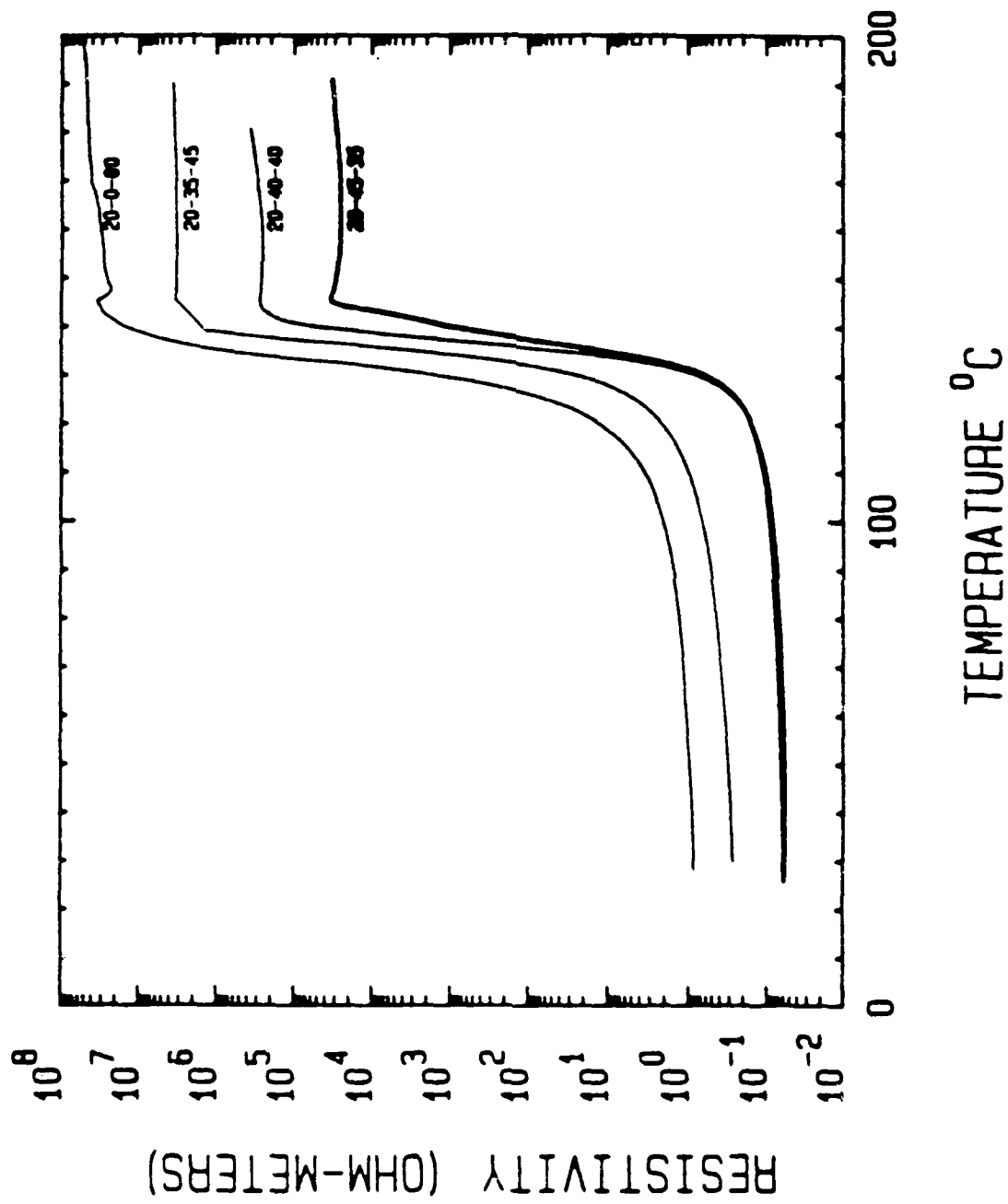


Figure 4.2.1 Resistivity-Temperature Curves for Triphasic Composites.

triphasic system appears to be 20 volume % carbon black-40 volume % Zeospheres-40 volume% PE. At this composition the lowest possible room temperature resistivity is coupled with a 7 order of magnitude change in resistivity.

The addition of mullite Zeospheres does in fact appear to sufficiently stabilize the structure and reduce carbon black motion in order to impede the onset of an NTC effect as well as prevent sample deformation at higher temperatures. The zeospheres also lower the room temperature resistivity due to the 3(0-3)-0 type of connectivity that exists in these triphasic composites, as discussed earlier. The 3(0-3)-0 connectivity also permits the mullite Zeospheres to decrease the overall thermal expansion of the composite (40,41) without drastically affecting the microscopic thermal expansion of the carbon black-PE quasi-phase. The expansion in this quasi-phase is what gives rise to the PTC effect.

To determine what effect the size of the insulating filler has on the PTC and high temperature characteristics, samples were prepared substituting the A-14  $\text{Al}_2\text{O}_3$  (4.0  $\mu\text{m}$ ) and the AKP-30  $\text{Al}_2\text{O}_3$  (0.42  $\mu\text{m}$ ) powders for the Zeospheres as the insulating phase. As seen in Figure 4.2.2, the composites with the different sized fillers still maintained the high post-PTC resistivity, but at the same carbon black and insulator concentrations exhibited considerable differences in the magnitude of the PTC and the room temperature resistivity.

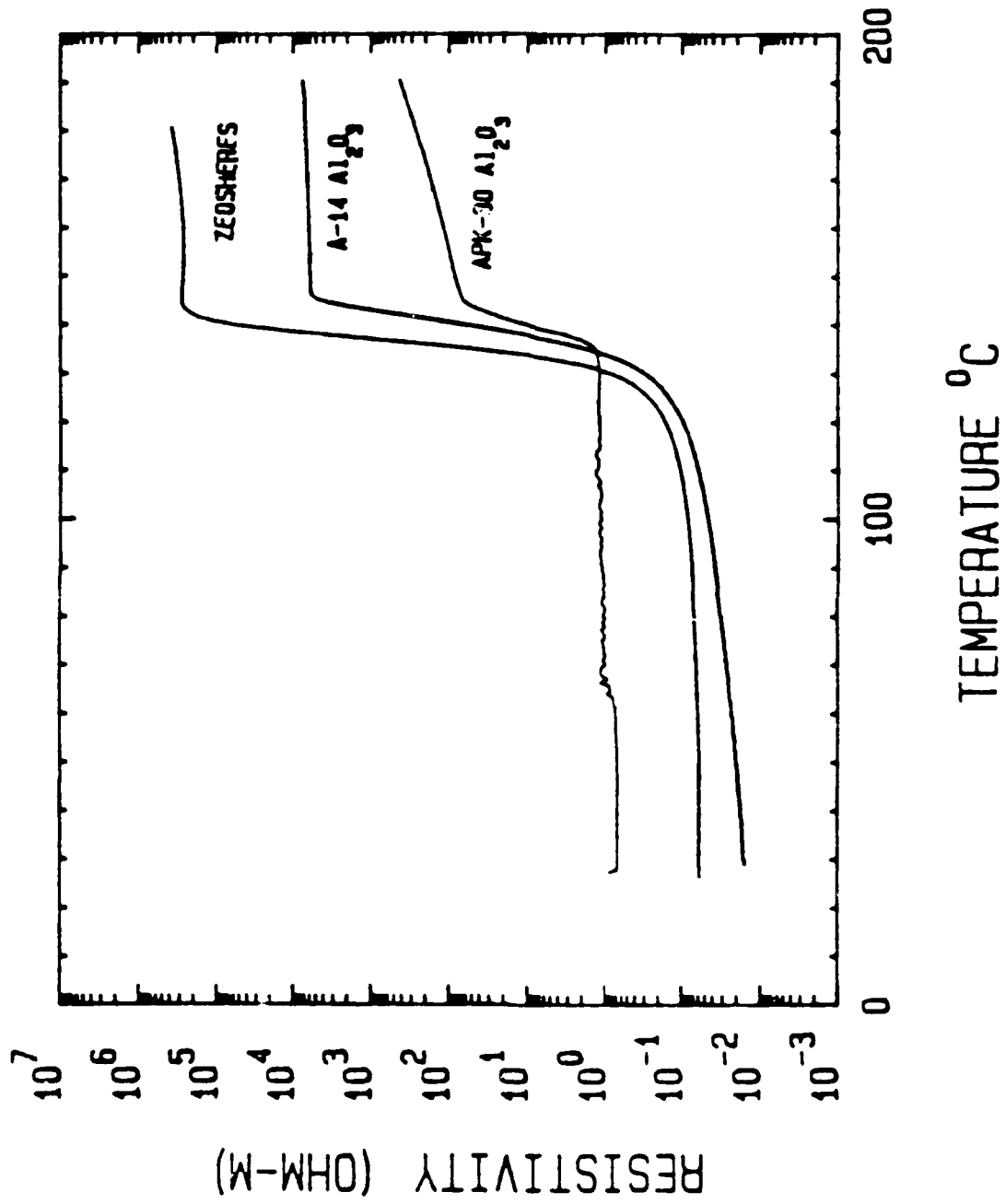


Figure 4.2.2 Resistivity-Temperature Curves for Triphasic Composites with Different Size Fillers.

The composite containing the A-14  $Al_2O_3$  exhibited a slightly lower room temperature resistivity and a moderately smaller PTC effect than the composites containing the Zeospheres. This behavior corresponds to the 3(0-3)-0 connectivity model described previously for the Zeospheres-carbon black system.

The composites using the AKP-30  $Al_2O_3$  as the insulating phase exhibited a much higher room temperature resistivity and a very small PTC effect. This is probably due to the smaller size of the AKP-30 particles. They only differ from the size of the carbon black particles by approximately one order of magnitude. The behavior of the AKP-30 composites corresponds to the behavior of a 0-0-3 type of connectivity. This accounts for the substantially higher room temperature resistivity as well as the reduced PTC effect. The decrease in magnitude of the PTC is the same effect shown in highly loaded diphasic samples. High filler concentrations hinder the motion of the conductor particles and make it more difficult to completely sever the conducting pathways. Hence, the resistivity does not increase to as high a value as samples with lower filler loadings.

#### 4.3 THERMAL CYCLING

To determine the reproducibility of both the diphasic

and the triphasic composites on thermal cycling, the resistivity was measured as a function of temperature on heating and cooling. The samples were subjected to a series of heating and cooling cycles between 25-190°C using the apparatus described in Section 2.4. The same heating and cooling rate of 4°C/minute was used throughout this study. All triphasic samples discussed contain zeospheres as the insulator phase.

As demonstrated in Section 4.2, the triphasic carbon black-insulator-PE composite system will exhibit PTC behavior similar to the crosslinked diphasic systems. The ability of both types of composites to withstand repeated "switching" or heating-cooling cycles is also important.

Figures 4.3.1 and 4.3.2 show a typical heating and cooling cycle for both a crosslinked and an uncrosslinked diphasic carbon black-PE composite. The non-crosslinked sample not only displays an NTC above the transition temperature on heating, but the cooling curve is drastically different from the heating curve, indicative of the large scale rearrangement of carbon black particles. Contact problems also arose on cooling due to sample deformation, causing discontinuities in the cooling curves.

In contrast, the cooling curve for the crosslinked composite is merely a shift of the heating curve. This hysteresis on cooling is due to inherent properties of the polymer. Polymer crystallization temperatures are generally lower than their melting temperatures because of the slow

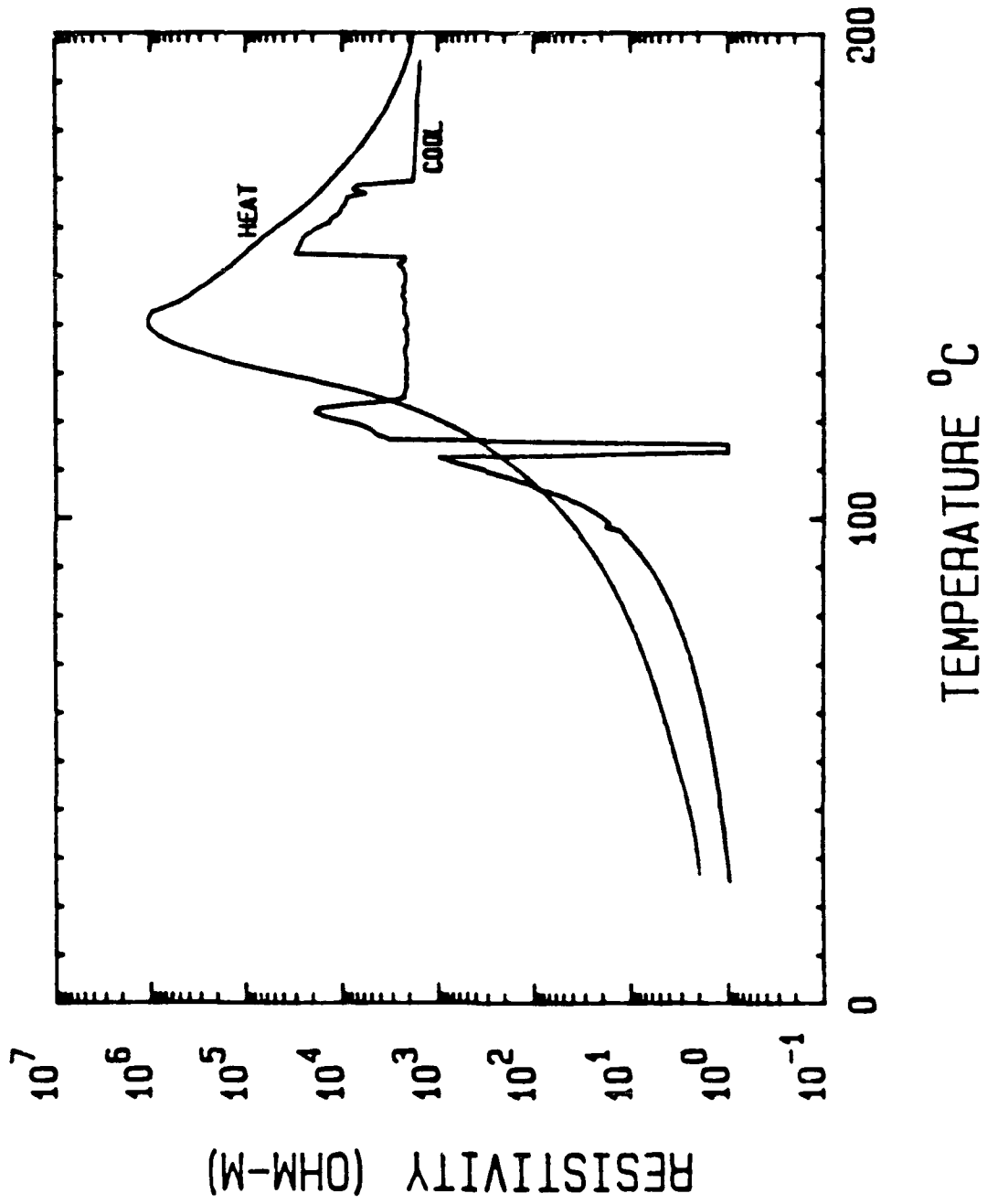


Figure 4.3.1 Heating-Cooling Curve for Uncrosslinked Sample.

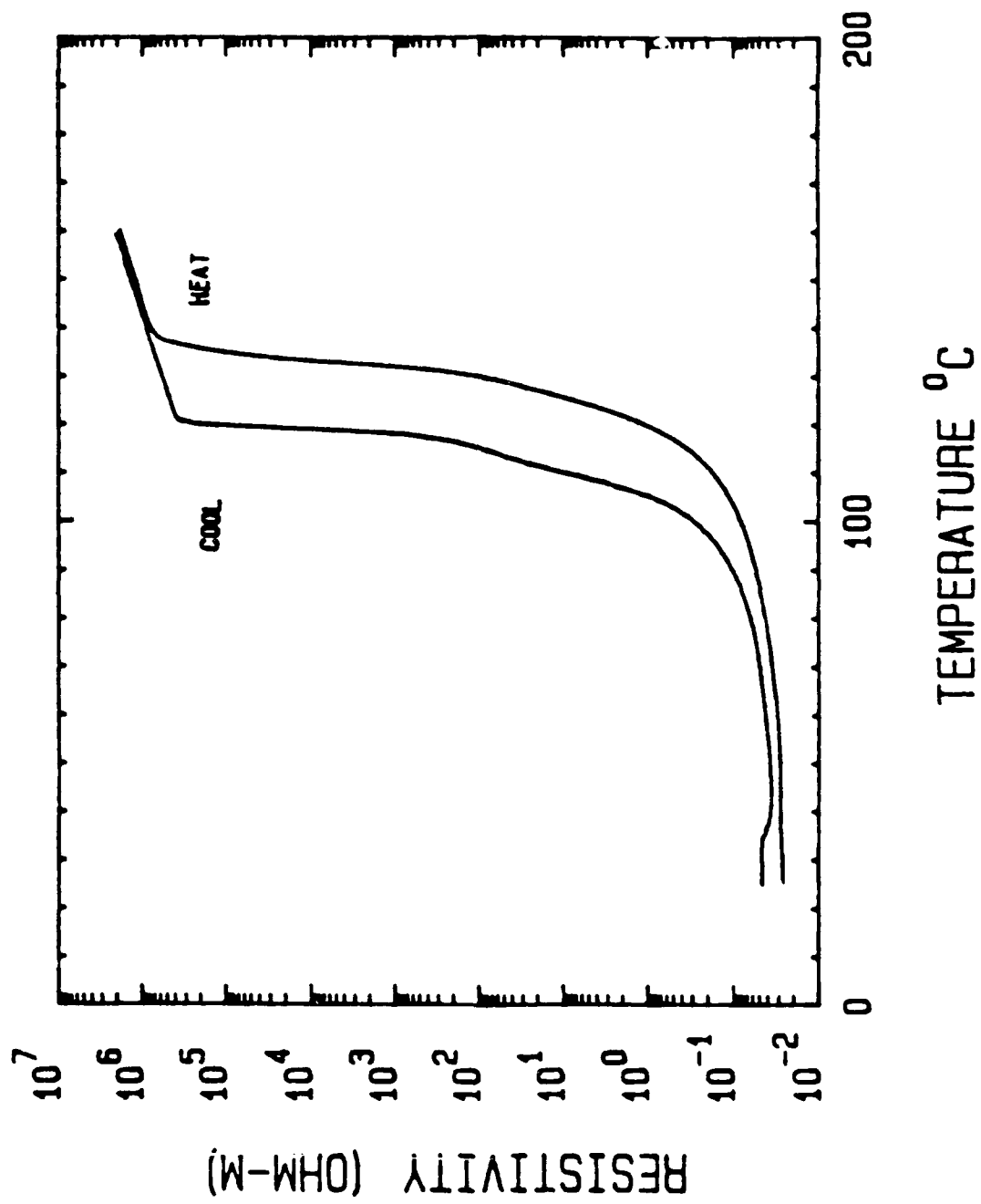


Figure 4.3.2 Heating-Cooling Curve for Crosslinked Sample.

crystallization kinetics and poor thermal conductivity.<sup>(43)</sup> Slower cooling rates (1°C/min) did not reduce this hysteresis.

A heating and cooling cycle for a 20-40-40 triphasic composite is shown in Figure 4.3.3. The cooling cycle is also an approximate shift of the heating curve, very similar to the crosslinked diphasic samples.

Figure 4.3.4 demonstrates the effect of multiple heating cycles on a typical crosslinked composite. The sample was subjected to three consecutive heating-cooling cycles. As cited in Section 1.5, the first cycle usually differs from subsequent cycles due to differences in thermal history. The second, third and subsequent cycles are virtually identical. A slight increase in the room temperature resistivity occurs due to the slow recovery time of these composites. Further discussion of the recovery time can be found later in this Section. A non-crosslinked composite, as shown in Figure 4.3.1, will exhibit drastic and irreversible changes between each heating cycle, and therefore is of little value as a thermistor.

Figure 4.3.5 shows the first, third, and fifth heating cycles of a 20-45-35 triphasic composite. Typical of these composites, the first cycle is slightly different, with slightly lower room temperature resistivity and lower peak PTC resistivity. Subsequent cycles give virtually identical results. A 20-40-40 triphasic composition also displays the same good thermal cycling characteristics, as seen in Figure

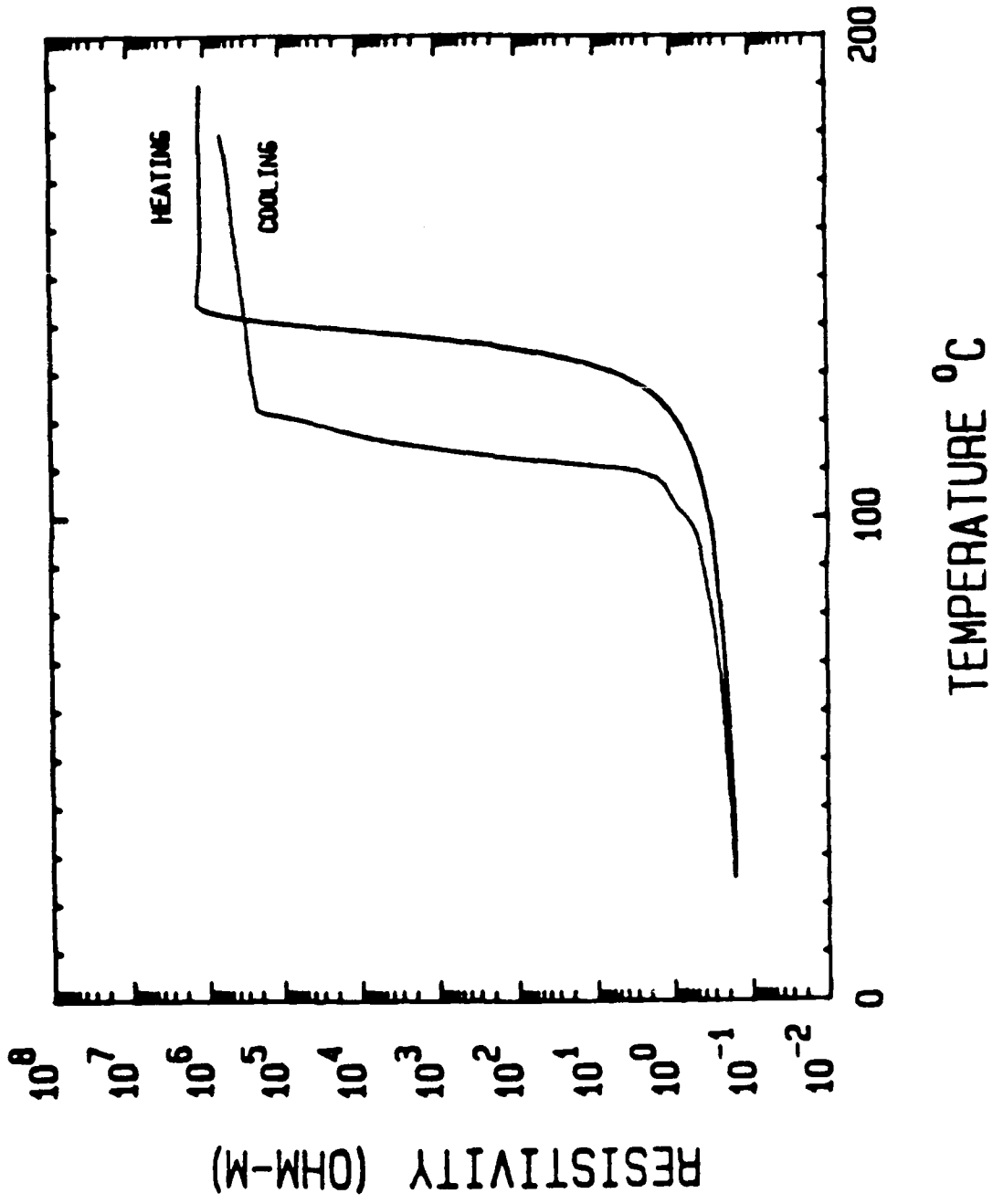


Figure 4.3.3 Heating-Cooling Curve for Triphasic Sample.

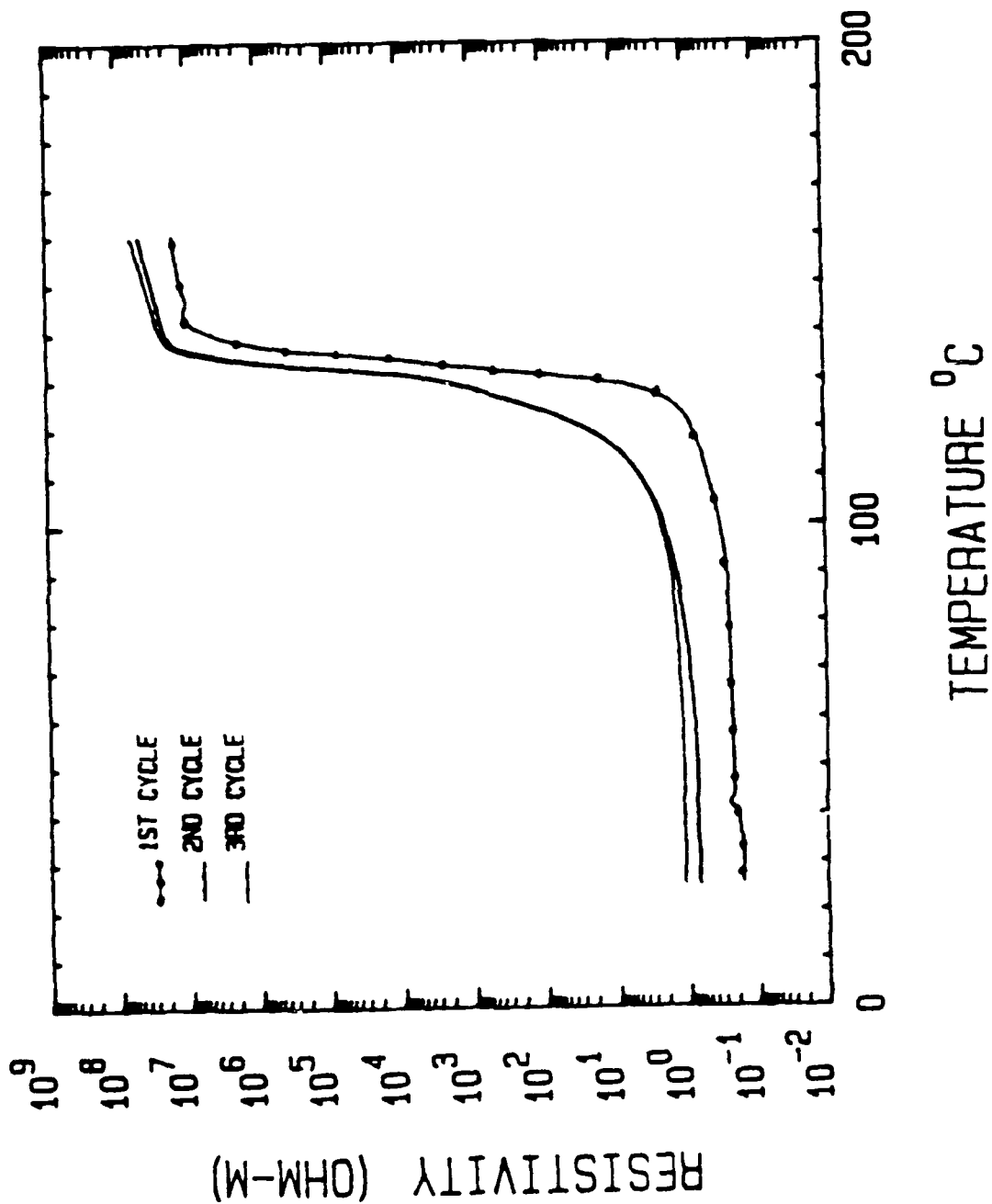


Figure 4.3.4 Multiple Heating Curves for a Crosslinked Composite.

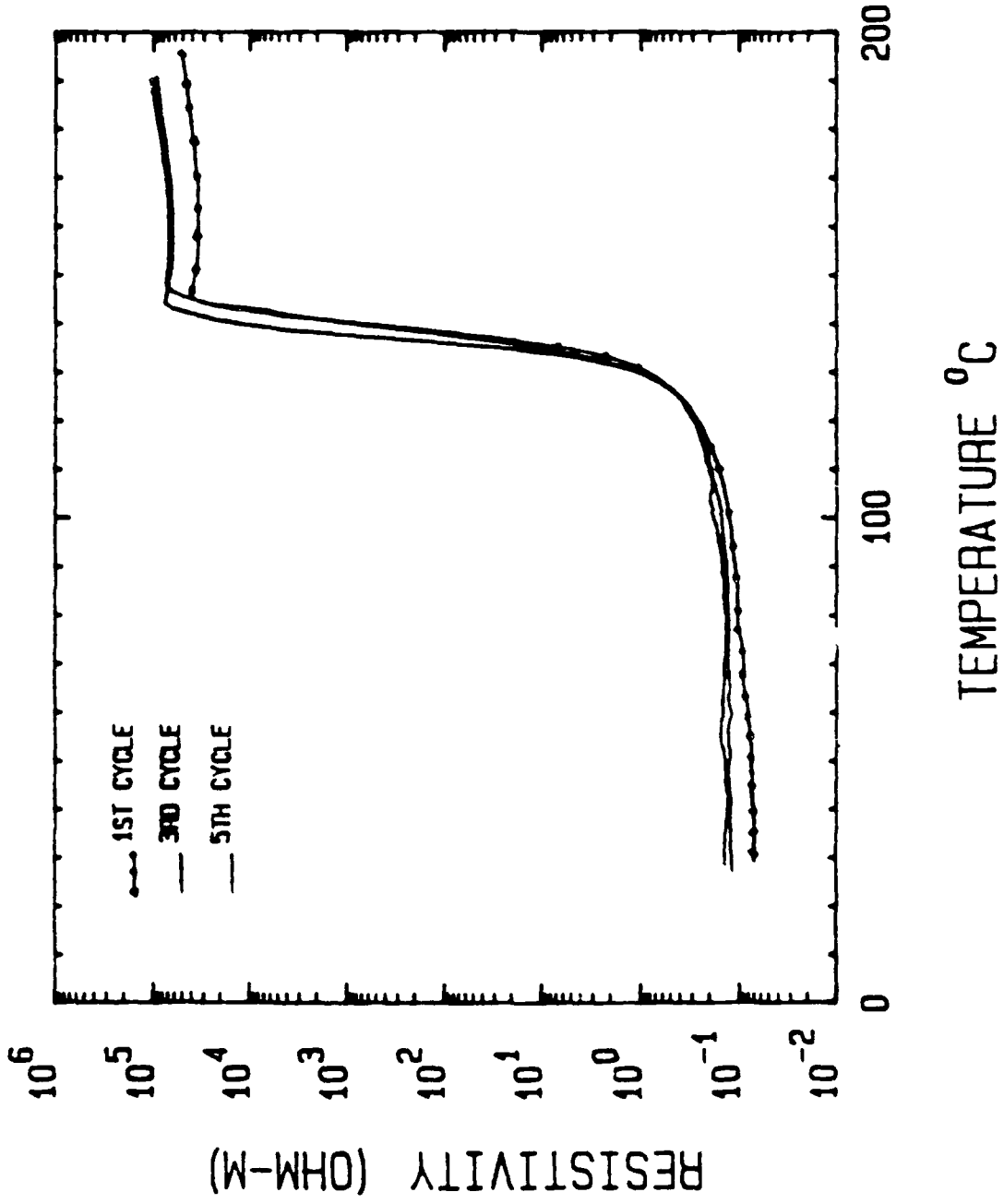


Figure 4.3.5 Multiple Heating Curves for a Triphasic Composite.

## 4.3.6.

As evidenced throughout the thermal cycling graphs, the sample resistivity does not return exactly to its pre-cycling value of resistivity after cycling. A certain amount of time is required for a sample to regain its base resistance. Recalling from Chapter 1, a composite will seldom return to its initial, pre-thermal cycling resistance. Instead, they usually return to a maximum base resistance, which is the resistance measured after the sample has undergone one thermal cycle.

Table 4.3.1 lists the results of a recovery time study.  $R(\text{INT})$  is the resistance of the sample prior to any thermal cycling. One thermal cycle consists of heating the sample to  $160^{\circ}\text{C}$  and then cooling it to  $25^{\circ}\text{C}$ . The resistance measured 24 hours after the first thermal cycle has been completed is called the base resistance  $R(\text{BASE})$ .  $R(0)$  is the resistance measured immediately following the completion of a subsequent thermal cycle.  $R(24)$  is the resistance measured 24 hours after the completion of a thermal cycle.

Raychem Corporation reports (1,2\*) that after the first thermal cycle, the Polyswitch device exhibits a resistance  $R(0)$  20% greater than the initial resistance  $R(\text{INT})$  of the device. After 24 hours, the Polyswitch thermistor has returned to a base resistance  $R(\text{BASE})$  15% greater than the initial resistance. Each subsequent cycle results in an  $R(0)$  approximately 5% larger than the base resistance. Within 24 hours, the resistance  $R(24)$  has returned to approximately

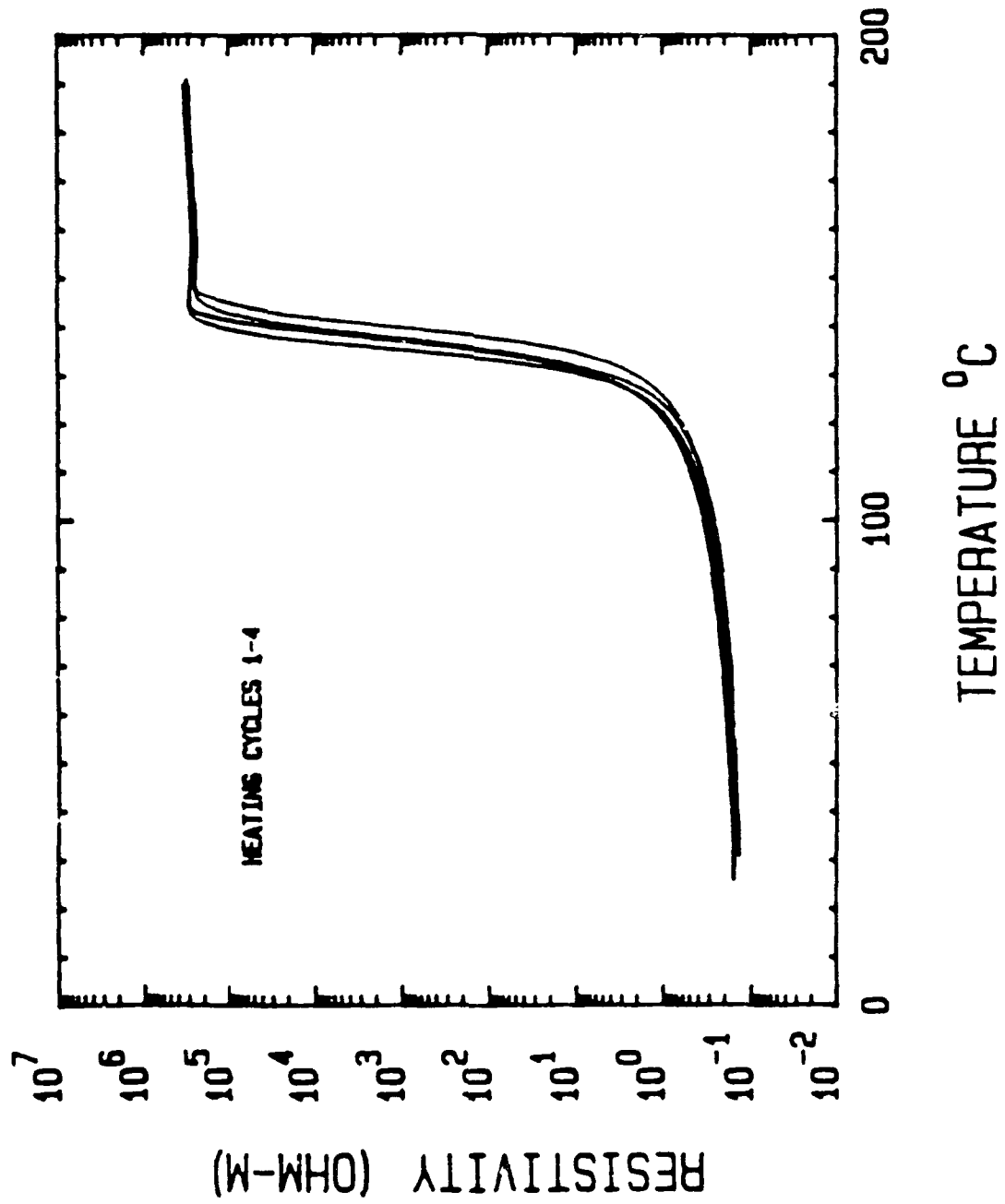


Figure 4.3.6 Multiple Heating Curves for a Triphasic Composite

Table 4.3.1 Typical Recovery Properties

Sample	R(BASE) [% > R(INT)]	R(0) [% > R(BASE)]	R(24) [% > R(BASE)]
Diphasic, Not crosslinked	39	22	11
Diphasic, Crosslinked	17	10	4
Ravchem Polyswitch(28)	15	5	R(BASE)
20-40-40	16	6	0.1
20-45-35	17	6	0.4

the base resistance.

Uncrosslinked samples show very large changes in resistance on each cycle, as stated previously. After 24 hours, they only returned to within 10-15 % of the base resistance. Crosslinked samples displayed greatly improved recovery properties but still showed somewhat larger changes in resistance than did the Raychem Polyswitch devices. The resistance measured 24 hours after cycling R(24) was still 4% greater than the base resistance. The reason for the discrepancy between the Raychem devices and samples produced at MRL is probably related to size. The Raychem Polyswitch device is much smaller, approximately one-fourth the size of the samples produced at MRL. A smaller sample size allows allows better heat dissipation and faster polymer recrystallization.

The triphasic samples gave results similar to the crosslinked samples. Immediately after cycling they exhibited a resistance 6-7% higher than the base resistance. After 24 hours, they had returned to within 1% of their base resistance. The recovery of the triphasic samples after 24 hours was somewhat better than the crosslinked samples. Because the recovery problem is rooted in the slow recrystallization process of PE, the lower volume fraction of PE combined with the presence of a good thermal conducting phase (mullite) may account for the better recovery properties of the triphasic composites. Also, larger amounts of filler may result in a greater number of

nucleation sites and therefore faster crystallization rates.

One problem that was encountered throughout the thermal cycling study was the degradation of the sample electrodes. The thermal expansion of the composite caused cracking, flaking, and bubbling of the silver electrodes during thermal cycling. The effect was especially prevalent in the diphasic samples, both crosslinked and uncrosslinked. Electrodes adhered much better to the triphasic composites, even after numerous cycles to 200°C. This is probably due to the presence of the insulator phase which decreases the overall thermal expansion of the composite sample.

#### 4.4 HIGH POWER TESTING

The results of preliminary high power testing of the carbon black-PE diphasic composites were obtained from Dr. Manfred Kahn at the Naval Research Laboratory in Washington D.C.. The maximum steady state voltages and the maximum pulse current were tested.

The maximum steady state voltage was determined by applying successively higher steps of D.C. voltage while monitoring the current at each step. The lowest voltage level at which the current does not stabilize is designated the "steady state runaway voltage".(44)

Samples with greater volume fractions of carbon black exhibit higher breakdown voltages. Samples containing 30

and 35 volume percent of carbon black have breakdown voltages in excess of 1000 V/mm. The higher breakdown strength of the composites with larger carbon black concentrations may be attributed to better current carrying capabilities due to the greater number of conducting pathways in the samples.

At the present time, the electrode system seems to be the limiting experimental factor. Several different types of electrode systems were tested, including evaporated aluminum, sputtered gold, silver neodecanate, and air dry silver. Evaporating aluminum and sputtering gold caused surface heating of the samples and resulted in the formation of a polymer film over the electrode surface. Silver paint cracked and flaked off under high voltages. A silver neodecanate solution decomposed in a wet oxygen atmosphere at 100°C was found to provide the best electrode to date for the high voltage testing.

#### 4.5 HIGH FREQUENCY MEASUREMENTS

Throughout this study, most of the resistivity versus temperature measurements were taken at a frequency of 1 KHz because the greatest PTC effects occurred at this frequency. To determine the maximum frequency at which these composites can be operated and still maintain a significant PTC effect resistivity versus temperature measurements were also taken

at frequencies of 10 KHz, 100 KHz, 1MHz, and 10 MHz.

Figures 4.5.1 and 4.5.2 illustrate the effect of frequency on both the diphasic and the triphasic composite systems. At temperatures above the PTC transition temperature, the resistivity decreases with increasing frequency due to Maxwell-Wagner effects.<sup>(2)</sup> As the frequency is increased, the magnitude of the PTC effect is reduced.

Although the decrease in high temperature resistivity with increasing frequency is predicted by Maxwell-Wagner models of conductor-insulator composites, at frequencies as high as 1 MHz the effect was expected to be much more drastic due to the relaxation of space charge effects. Surprisingly, a 4 order of magnitude change in resistance is still visible at a frequency of 1 MHz.

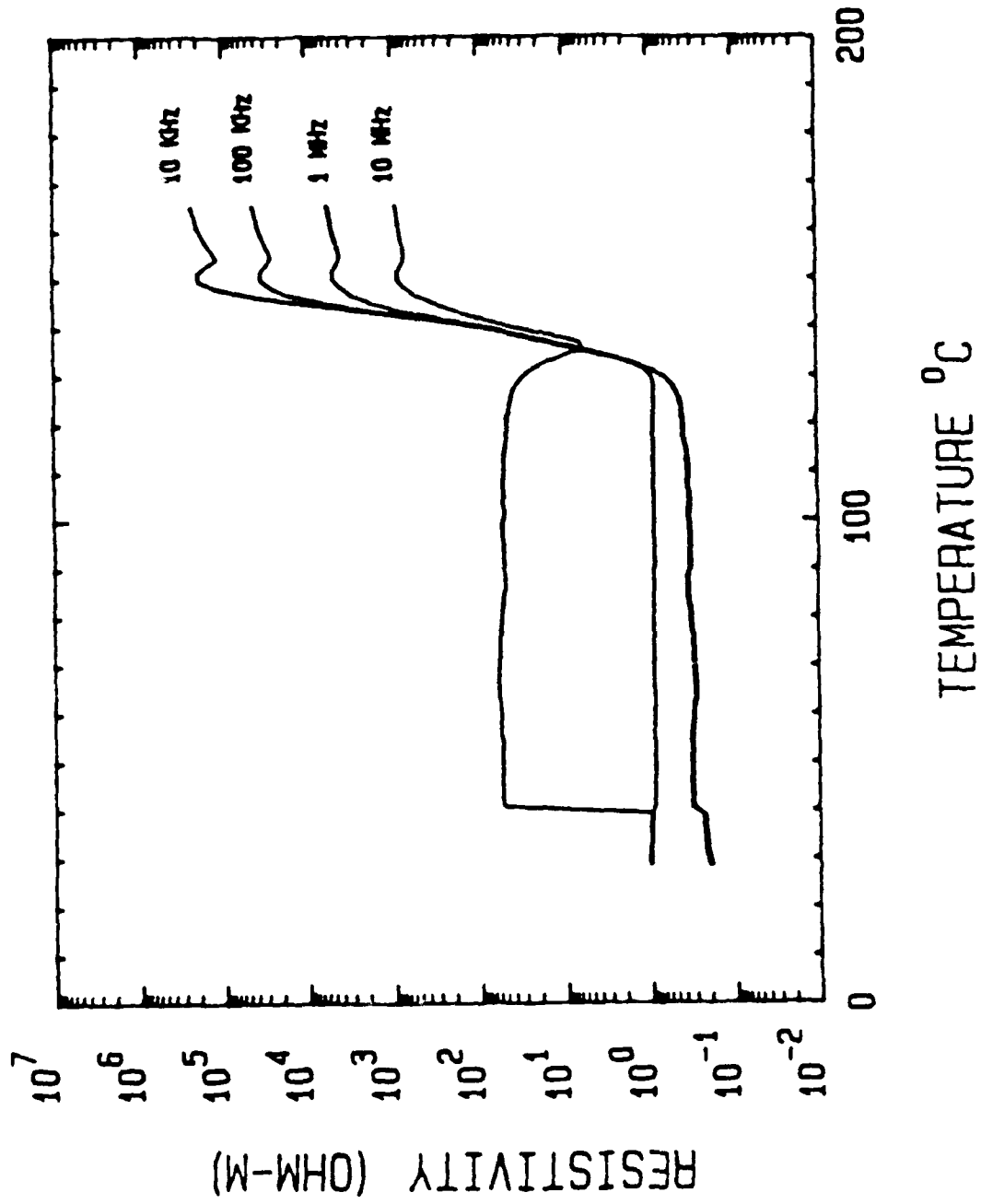


Figure 4.5.1 Resistivity-Temperature Curve for a Crosslinked Diphasic Composite at Various Frequencies.

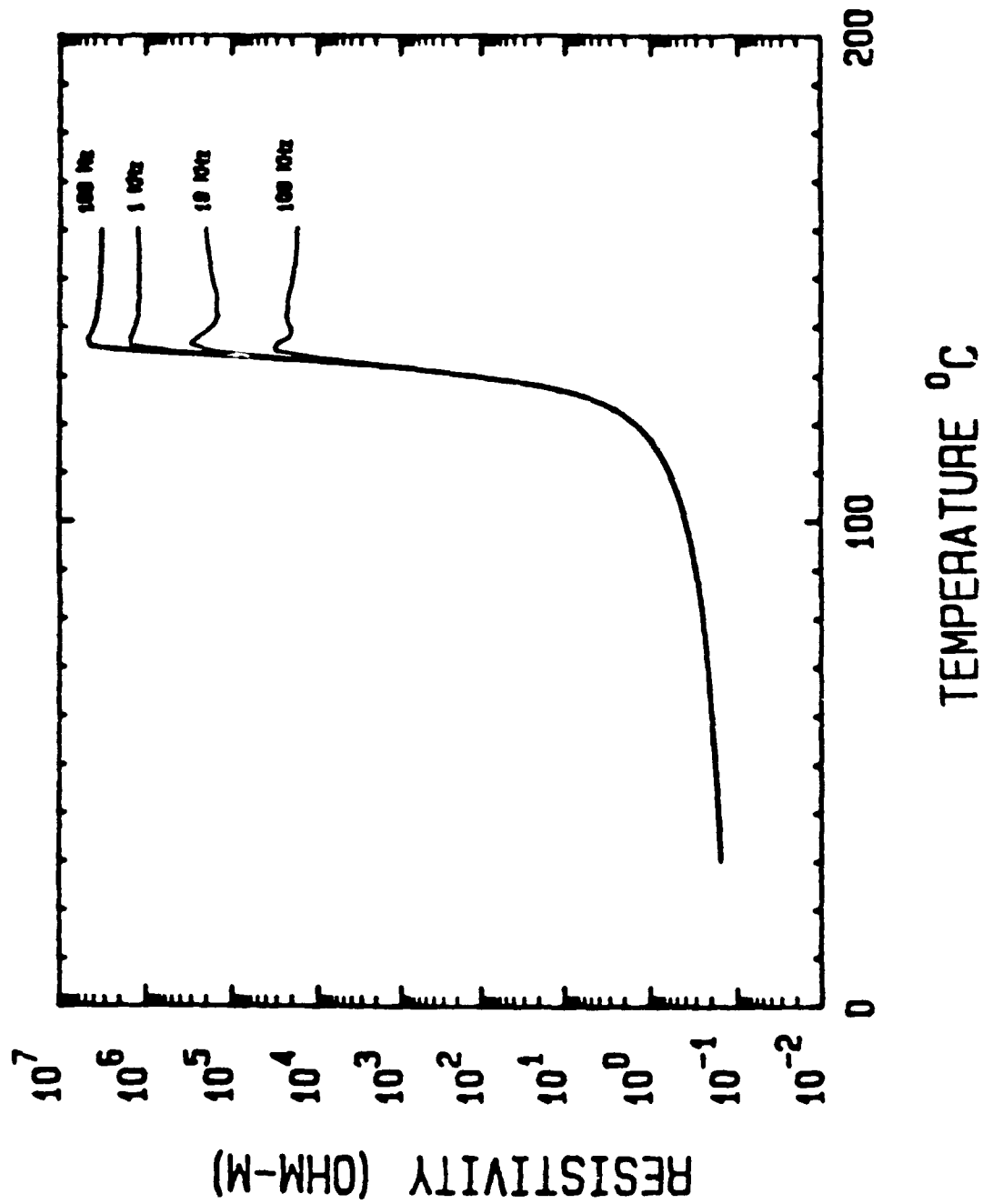


Figure 4.5.2 Resistivity-Temperature Curve for a Triphasic Composite at Various Frequencies.

## CHAPTER FIVE

## SUMMARY AND CONCLUSION

Until recently, most PTC thermistors were composed of a rare earth doped  $\text{BaTiO}_3$ . Now a new class of composite thermistors also exists. Because the new composite thermistors offer many advantages over  $\text{BaTiO}_3$ , it is of interest to explore new and better methods of producing these composite materials and improving their properties.

The focus of this study was threefold. First, a new method of producing PTC thermistors that did not require crosslinking of the composite was explored. Second, the effects of a third filler on the percolation and PTC behavior of the composite was examined. Lastly, connectivity models were developed to explain the effects observed when a third filler was incorporated into the composite.

## 5.1 CONCLUSIONS

Diphasic carbon black-PE composites, similar to those commercially produced by Raychem Corporation, were prepared and resistivity measurements taken. Uncrosslinked samples

displayed poor thermistor characteristics, including an NTC effect and sample deformation at temperatures just above the PTC transition temperature. They also exhibited poor reproducibility of resistivity with thermal cycling. On the other hand, crosslinked samples did not display an NTC effect and maintained mechanical integrity above the PTC transition temperature. The crosslinked composites also showed good reproducibility on thermal cycling.

To eliminate crosslinking of the samples, a third insulator phase was added to the composite to stabilize the structure and inhibit the motion of carbon black particles. The triphasic composites displayed the same substantial PTC effect as the diphasic samples without the subsequent NTC effect. The thermal cycling properties of the triphasic composites matched or exceeded those of the crosslinked diphasic composites. In addition, electrodes adhered better to the triphasic samples on thermal cycling, probably because of the lower thermal expansion of the triphasic samples.

Incorporating a third filler into the composite also had a profound effect on the percolation behavior of the composite. Adding the insulator phase resulted in a shift of the percolation curve. Shifts to both higher and lower resistivities have been observed, depending on the size of the filler.

The direction in which the percolation curve shifts has been correlated to the type of connectivity formed in the

composite. The type of connectivity formed is determined by the size difference between the conductor and the insulator. It has been proposed that when the insulator is approximately two orders of magnitude larger than the conductor, a quasi-composite with 3(0-3)-0 connectivity is formed.<sup>(\*)</sup> When the conductor and insulator are of the same order of magnitude in size, a 0-0-3 connectivity is believed to exist. The 3(0-3)-0 connectivity model predicts a decrease in resistivity of the composite upon addition of the insulating filler. A 0-0-3 connectivity suggests an increase in resistivity when the insulator is added. These predicted trends were confirmed by data presented in Chapter 3.

Both the diphasic and the triphasic composites were tested at frequencies up to 10 MHz. Both types of composites showed a decrease in the resistivity above the transition temperature, as expected. Surprisingly, the diphasic and the triphasic samples still exhibited modest PTC effects of about four orders of magnitude at frequencies as high as 1 MHz.

Preliminary results of the high power tests indicate that these composite thermistors could be useful as pulse power switches.

## 5.2 FUTURE WORK

One area that has shown promise for future work is the high frequency applications. Determining what conduction mechanisms are occurring at high frequencies might aid in determining the conduction mechanisms present at lower frequencies for this and other composite systems. Possible new applications for a high frequency PTC thermistor could be explored.

Another area for further research is high pulse power switching uses. These composite materials appear suitable for pulse power switches.<sup>(44, 45)</sup> Determination of the breakdown mechanisms could be useful in finding ways to improve the power handling capabilities of these composites.

Time delay PTC thermistors are another possible area of new research. By adding a third filler with a very high heat of fusion, the composite may be maintained at a temperature a few degrees above the PTC transition temperature. This would prevent the temperature of the composite from continuing to increase, thus preventing the NTC effect and sample deformation.

## REFERENCES

1. J.R. Carlson, "Thermistors for Overcurrent Protection," reprint from Machine Design, Dec. 10, 1981.
2. A.V. Medalia, "Electrical Conduction in Carbon Black Composites," Rubber Chem. Technol., 59(3) 432-454 (1986).
3. E.K. Sichel, Carbon Black-Polymer Composites: The Physics of Electrically Conducting Composites, Marcel Dekker, Inc., New York (1982).
4. R.E. Newnham, D.P. Skinner, and L.E. Cross, "Connectivity and Piezoelectric-Pyroelectric Composites," Mat. Res. Bull., 13, 525-536 (1978).
5. S.M. Pilgrim and R.E. Newnham, "3:0: A New Composite Connectivity," Mat. Res. Bull., 21, 1447-1454 (1986).
6. S.M. Pilgrim, R.E. Newnham, and L.L. Rohlfing, "An Extension of the Composite Nomenclature Scheme," Mat. Res. Bull., 22, 677-684 (1987).
7. R. Zallen, "The Percolation Model," The Physics of Amorphous Solids, Ch.4, 135-204, John Wiley & Sons, New York (1981).
8. C. Rajagopal and M. Satyam, "Studies on Electrical Conductivity of Insulator-Conductor Composites," J. Appl. Phys., 49(11), 5536-5540 (1978).
9. E.M. Abdel-Bary, M. Amin, and H.H. Hassan, "Factors Affecting Electrical Conductivity of Carbon Black-Loaded Rubber. II. Effect of Concentration and Type of Carbon Black on Electrical Conductivity of SBR," J. Polym. Sci., 17, 2163-2172 (1979).
10. D.M. Bigg, "An Investigation of the Effect of Carbon Black Structure, Polymer Morphology, and Processing History on the Electrical Conductivity of Carbon-Black-Filled Thermoplastics," J. Rheol., 28(5), 501-516 (1984).

11. R.L. McCullough, "Generalized Combining Rules for Predicting Transport Properties of Composite Materials," Center for Composite Materials and Department of Chemical Engineering, University of Delaware, Newark, Delaware 19716.
12. M. Narkis and A. Vaxman, "Resistivity Behavior of Filled electrically Conductive Crosslinked Polyethylene," J. Appl. Polym. Sci., 29, 1639-1652 (1984).
13. K. Miyasaka, K. Watanabe, E. Jojima, H. Aida, M. Sumita, and K. Ishikawa, "Electrical Conductivity of Carbon-Polymer Composites as a Function of Carbon Content," J. Mat. Sci., 17, 1610-1616 (1982).
14. R.D. Sherman, L.M. Middleman, and S.M. Jacobs, "Electron Transport Processes in Conductor-Filled Polymers," Polym. Eng. Sci., 23(1), 36-46 (1983).
15. R.H. Norman, Conductive Rubbers and Plastic, Applied Science Publishers, London (1970).
16. M. Narkis, A. Ram, and F. Flashmer, "Electrical Properties of Carbon Black Filled Polyethylene," Polym. Eng. Sci., 18(8), 649 (1978).
17. L.V. Azaroff and J.J. Brophy, Electronic Processes in Materials, McGraw-Hill, New York (1963).
18. R.M. Scarisbrick, J. Phys. D, 6 2098 (1973).
19. L. Benguigui, J. Yacubowicz, and M. Narkis, "On the Percolative Behavior of Carbon Black Cross-Linked Polyethylene Systems," J. Polym. Sci., 25, 127-135 (1987).
20. P.V. vanKonynenburg, A. Au, C. Rauwendaal, and A.J. Gotcher, "Low Resistivity PTC Composites," Raychem Corp., Menlo Park, Calif., U.S. Patent #4,237,441, Dec. 2, 1980.
21. J.M. Taylor, "Devices Containing PTC Conductive Polymer Compositions," Raychem Corp., Menlo Park, Calif., U.S. Patent #4,426,633, Jan. 17, 1984.

33. Manufacture's information included with shipment.
34. R.J. Pugh and F.M. Fowkes, "The Dispersibility and Stability of Carbon Black Media of Low Dielectric Constant. 2. Sedimentation Volume of Concentrated Dispersions, Adsorption and Surface Calorimetry Studies," Colloids and Surfaces, 9, 33-46 (1984).
35. Zeospheres data sheet, Zeelan Industries Inc.
36. Cabot Technical Report S-36, October 1984.
37. Cabot Technical Report.
38. S. Radhakrishnan, "Effect of a Third Component on the Electrical Properties of Conducting Polymer Composites," J. Mat. Sci. Letters, 4, 1445-1448 (1985).
39. H. Banno, "Recent Developments of Piezoelectric Ceramic Products and Composites of Synthetic Rubber and Piezoelectric Ceramic Particles", IEEE International Symposium on Applications of Ferroelectrics, Gaithersburg, MD. June 1-3, 1983.
40. S. Radhakrishnan, "Curing Behavior of Conducting Polymer Composite," J. Mat. Sci. Letters, 6, 145-148 (1987).
41. S.K. Bhattacharya and A.C.D. Chaklader, "Review on Metal-Filled Plastics. Part 2. Thermal Properties," Polym.-Plast. Technol. Eng., 20(1) 35-59 (1983).
42. R.B. Seymour, C.E. Carraher, Structure-Property Relationships in Polymers, Plenum Press, New York (1984).
43. I.I. Perepechko, An Introduction to Polymer Physics, Mir Publishers, Moscow (1981).
44. R.D. Ford and M. Kahn, "Positive Temperature Coefficient Resistors as High Power Pulse Switches: Performance Limitations, Temperature Effects and Triggering Behavior", Naval Research Laboratory, Washington D.C. Report 20375-5000.

45. R.D. Ford, I.M. Vitkovitsky, and M. Kahn, "Application of Non-Linear Resistors to Inductive Switching", IEEE Transactions on Electrical Insulation, Vol.EI-20 No.1. 29-37 (1985).